

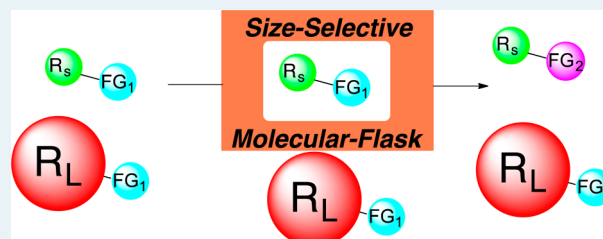
Size-Selective Molecular Flasks

Matthias Otte*

Organic Chemistry & Catalysis, Debye Institute for Nanomaterials Science, Universiteit Utrecht, Universiteitsweg 99, 3584 CG Utrecht, The Netherlands

ABSTRACT: Molecular flasks are compounds that are able to mediate or catalyze chemical transformations inside their cavities. The development of such compounds is often inspired by nature. Enzymes, nature's catalysts, are able to convert a certain substrate with very high turnover number and selectivity. In addition to their very high chemo-, regio-, and stereoselectivity, enzymes are also able to distinguish their substrates on the basis of size, resulting in size selectivity. To date, many synthetic materials such as metal–organic frameworks are used to accomplish size-selective transformations. However, also the number of molecular flasks known to mediate or catalyze size-selective transformations is increasing. In this perspective an overview on classic and the most recent examples of size-selective molecular flasks is given. In addition, an outlook on promising developments in cavity chemistry that may lead to the development of additional size-selective molecular flasks is given.

KEYWORDS: size-selective catalysis, cavities, supramolecular chemistry, organic cages, confined space



I. INTRODUCTION

Since the pioneering work of Cram,¹ Lehn,² Pedersen,³ and Vögtle⁴ the design of molecular architectures, offering cavities of defined size and functionalization, has become an exciting and highly pursued field in modern synthetic chemistry. Examples are macrocyclic and cage-type compounds. Early reports by Rebek,⁵ Stang,⁶ and Fujita⁷ illustrate that the synthesis of such compounds can be favored through thermodynamically controlled reaction pathways, enabling their formation via self-assembly phenomena. In addition, the use of templates, as shown for example by Sanders and Anderson,⁸ can favor one architecture over others, even if the bond-forming reactions occur under kinetic control. These tools have motivated chemists to constantly extend the library of functional cavities, leading to new and topologically versatile architectures.⁹ In addition to the curiosity to establish new topological motifs, applications of functionalized molecular cavities have been frequently investigated. Examples are their use as sensors to selectively encapsulate a certain compound,¹⁰ for gas storage,¹¹ or as molecular switches.¹² Moreover, cavities have been shown to be capable of storing highly reactive compounds in a safe manner via encapsulation.¹³

Inspired by enzymatic reactive sites, which are located in confined spaces, resulting in high selectivities and turnover numbers for given reactions, the development of molecular compounds, which offer cavities that can mediate or catalyze transformations has become of great interest. Such compounds are often called “molecular flasks”.¹⁴ The first example of a molecular flask that can catalyze a chemical transformation was reported by Rebek and co-workers in 1998.¹⁵ They used a purely organic cage compound that assembles via hydrogen-bonding interactions, a so-called “hydroxy softball”, to catalyze the Diels–Alder reaction between *p*-benzoquinone and a

thiophene dioxide derivative. Since then, much effort has been spent on the development of new molecular flasks.¹⁴ Molecular flasks offer a confined space where the chemical transformation takes place. This environment can have significantly different properties in comparison to the bulk reaction mixture, leading to an unprecedented reaction outcome. Examples are different regioselectivities¹⁶ or chemoselectivities¹⁷ and increased stereoselectivities.¹⁸ In addition, bringing reactants in the confined space close together can result in a large rate enhancement in comparison to the bulk reaction mixture.¹⁹ Moreover, the turnover number of the encapsulated catalyst can be significantly increased, resulting in cases where nearly unreactive compounds become active catalysts through encapsulation.²⁰

In addition to the aforementioned remarkable opportunities that catalysis in confined molecular spaces offer, there is a further advantage. This is the ability to act as a size-selective catalyst, meaning that the selective conversion of one substrate over others is based on their size. Size-selective reactions are of key importance if the desired substrates are in mixtures of compounds with similar chemical and physical properties. Examples are selective transformations of substrates from crude oil or biomass. Size selectivity is well established for materials such as metal–organic frameworks, zeolites, and covalent organic frameworks.²¹ However, also the number of reported molecular flasks acting as size-selective catalysts has been increasing in recent years. Size selectivity is thereby often achieved via installing cage pores of a defined size. Due to these pores, only substrates of a defined size are able to enter the cavity, which is the place where the transformation happens.

Received: June 23, 2016

Revised: August 16, 2016

Published: August 17, 2016

In this regard, to achieve a size-selective molecular flask behavior, the cavity must be able to mediate or catalyze a given transformation while the pores are responsible for selecting one substrate over others.

In this perspective, the development of size-selective catalysis in molecular flasks is described. The approach chosen here will discuss the molecular flasks on the basis of the nature of their cavity, including cavities obtained via metal–organic coordination, organic supramolecular interactions, and organic covalent cavities. Afterward an outlook on possible further concepts to obtain new size-selective molecular flasks will be given. Notably, size-selective reactions that are mediated or catalyzed by polymeric heterogeneous catalysts such as zeolites and metal–organic frameworks will not be discussed in this perspective.

II. METAL–ORGANIC COORDINATION CAVITIES

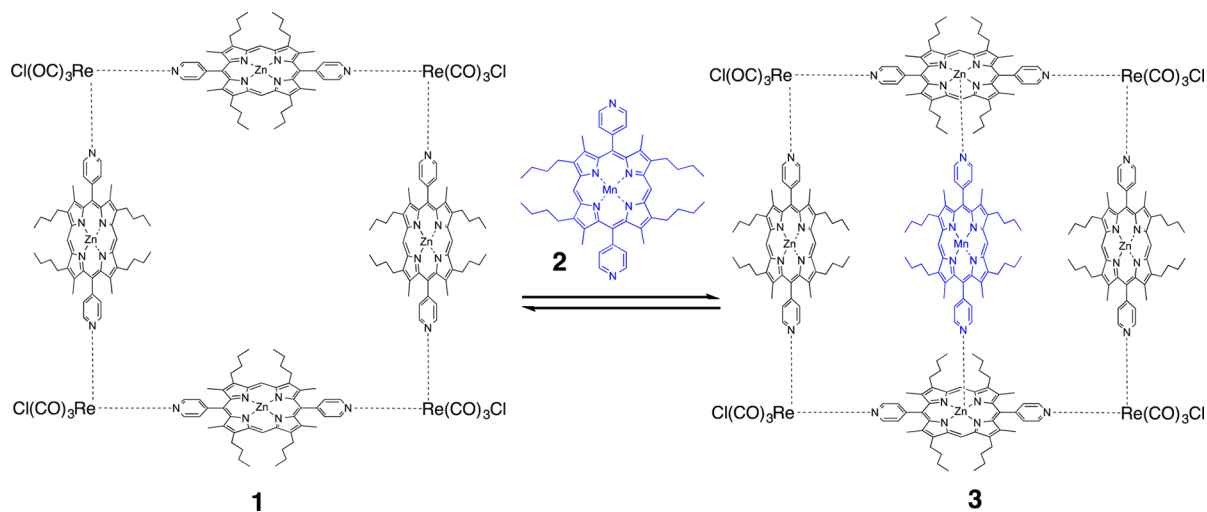
Cavities that are based on metal–organic coordination have been frequently investigated.^{22,23} Those architectures are often synthesized in high yields by mixing the building blocks in the right stoichiometric ratios. These high yields are caused by metal–ligand coordination that leads via self-assembling phenomena to the desired compounds. Different geometries can selectively be obtained via modification of the metal ions, bonding angles at the ligands, or changes in the solvent. Many molecular flasks that have been reported are based on metal–organic coordination.²⁴ Prominent examples stem from the groups of Fujita^{16a,b,25} and Toste, Bergman, and Raymond.^{17,26}

Cavities that are based on metal–organic coordination have also been reported to be size-selective molecular flasks.

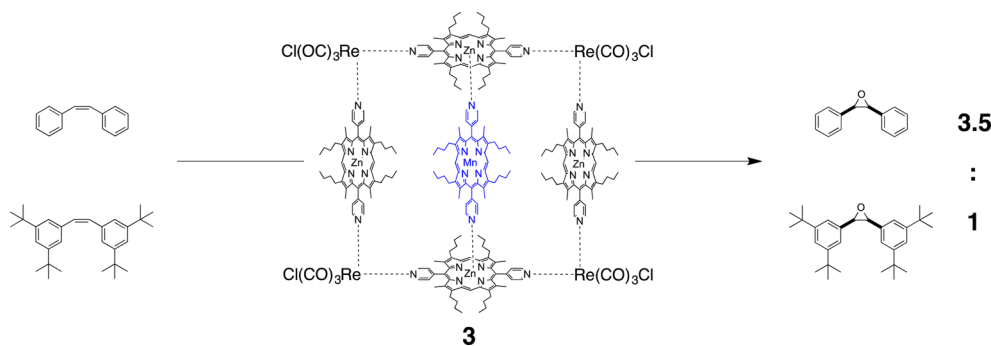
In 2001 Nguyen and Hupp reported macrocycle **1**, which assembles via coordination of four zinc dipyridine-porphyrins (Zn-DPyP) to four $\text{Re}(\text{CO})_3\text{Cl}$ groups.²⁷ Thereby each Zn-DPyP coordinates via its pyridine moieties to two different $\text{Re}(\text{CO})_3\text{Cl}$, resulting in a square-shaped cavity. The square-shaped cavity of this macrocycle is sufficiently large to encapsulate an additional manganese dipyridine-porphyrin (Mn-DPyP, **2**). This occurs via coordination of the pyridine moieties in **2** to the zinc ions, resulting in the formation of **3** (Scheme 1). It has been shown that **3** is a molecular flask able to catalyze the epoxidation of olefins.

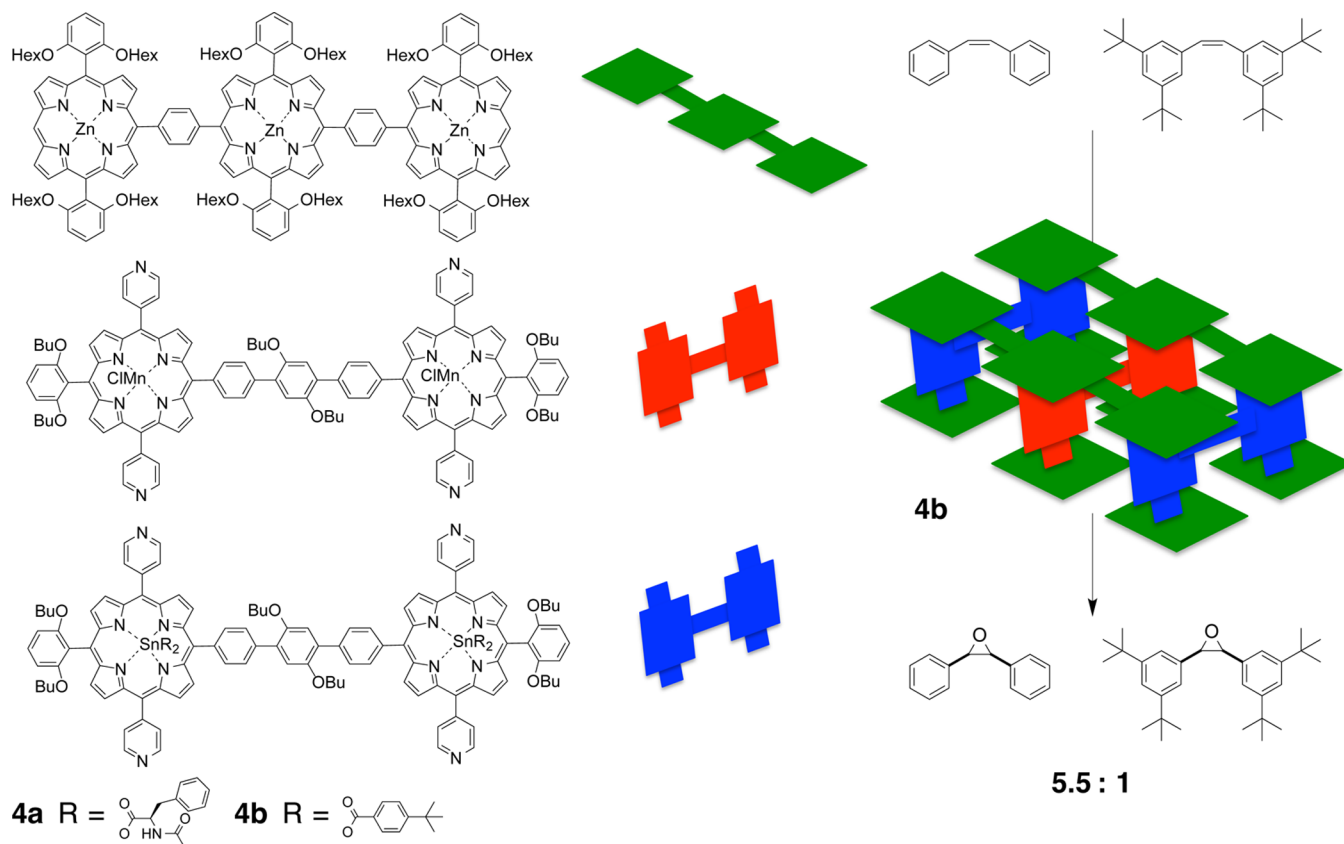
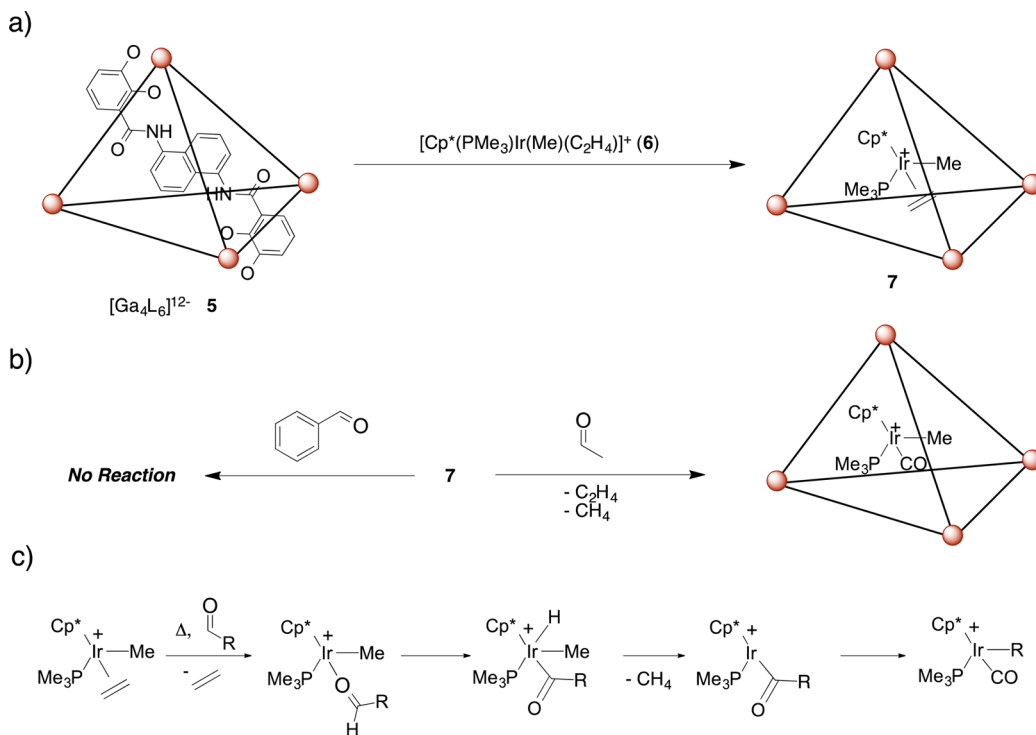
When iodosylbenzene was used as the oxidant, **3** showed a 10-fold higher turnover number (TON) for the epoxidation of styrene in comparison to free **2**. Further reduction of the concentration of **2**, with the concentration of **1** kept constant, resulted in even higher TONs of 7000. One deactivation pathway for manganese porphyrin catalyzed epoxidation reactions is the formation of Mn–O–Mn species that could be suppressed via the formation of **3**. In addition to its higher TON, **3** has also been shown to selectively convert substrates on the basis of their size. For example, *cis*-3,3',5,5'-tetra-*tert*-butylstilbene is 3.5 times less reactive with **3** in comparison to the sterically less demanding *cis*-stilbene (Scheme 2). Size-selectivity experiments were carried out at room temperature and in dichloromethane, using a 1:1 mixture of both olefins in the presence of 1 equiv of oxidant and 1 mol % of **3**. The size

Scheme 1. Synthesis of **3** via Encapsulation of Mn(DPyP) (**2**) in Self-Assembled Macrocycle **1**²⁷



Scheme 2. Size-Selective Epoxidation of *cis*-Stilbenes Catalyzed by **3**²⁷



Scheme 3. Schematic Representation of Size-Selective Catalysis with Torsionally Rigid, Self-Assembled Porphyrin Box 4b²⁹Scheme 4. (a) Synthesis of Host–Guest Complex 7, (b) Size-Selective C–H Bond Activation of Aldehydes by Host–Guest Complex 7, and (c) Mechanism of the C–H Bond Activation with Aldehydes³¹

selectivity could be increased by 7 times via coencapsulation of two 3,5-dinitrobenzoic acid dimethyl ester molecules (30–300 mol %). The two bulky esters coordinate via their

pyridine moieties to the remaining two zinc ions. This results in a reduced effective cavity size that is responsible for the higher size selectivity.

Although the coencapsulated ester is chiral and enantiomerically enriched, no enantiomeric excess (ee) was observed. The possibility that the macrocycle can adopt conformations where the chiral information points to the exterior instead to the cavity was considered the reason for the absence of enantioselectivity. This inspired Nguyen and Hupp to develop new systems based on cavity-tailored porphyrin boxes (Scheme 3).²⁸ These boxes assemble via coordination of 2 equiv of tin porphyrin dimers (blue cartoon) to 4 equiv of a zinc porphyrin trimer (green cartoon). Similar to the formation of 3, here pyridine–metal interactions are responsible for the cavity assemblies. After encapsulation of a manganese porphyrin dimer (red cartoon) the boxes became active catalysts for enantioselective thioether oxidation (4a) and the size-selective epoxidation (4b) of olefins.²⁹ Methyl *p*-tolyl sulfide has been shown to be oxidized by 4a, resulting in methyl *p*-tolyl sulfoxide, which has been obtained with an ee of up to 14%. Although this ee is moderate, Nguyen and Hupp stated that 4a and its further reported derivatives are the first instances where chiral environments surrounding active sites in abiotic supramolecular assemblies have been shown to induce enantioselection by an achiral catalyst.

In addition to the observed enantioselectivity that could be accomplished by 4a, modification of the tin porphyrin dimer resulted in the formation of 4b. 4b is able to act as a size-selective catalyst. It has been shown that *cis*-stilbene is 5.5 times more reactive with 4b in comparison to the sterically demanding *cis*-3,3',5,5'-tetra-*tert*-butylstilbene (Scheme 3).

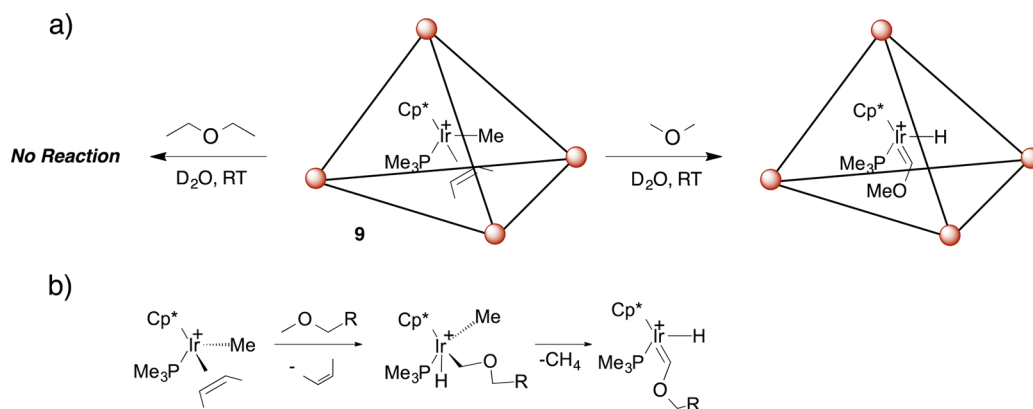
The synthesis of M_4L_6 tetrahedral cage compounds ($M = \text{Ga}, \text{Fe}$, $L = N,N'$ -bis(2,3-dihydroxybenzoyl)-1,5-diaminonaphthalene) was described by Raymond in 1998.³⁰ Here, one metal ion is located in each corner of the tetrahedron (Scheme 4a). Each metal ion is coordinated by three bidentate moieties that belong to three different ligands. Each ligand coordinates to two different metal ions, resulting in the overall tetrahedral assembly.

Ga_4L_6 (5) has been shown to be a suitable host for transition-metal complexes such as $[\text{Cp}^*(\text{PMe}_3)\text{Ir}(\text{Me})(\text{C}_2\text{H}_4)]^+$ (6), resulting in the host–guest complex 7 (Scheme 4a).³¹ In bulk reaction mixtures, 6 is able to activate the C–H bonds of aldehydes such as acetaldehyde and benzaldehyde, resulting in $[\text{Cp}^*(\text{PMe}_3)\text{Ir}(\text{Me})(\text{CO})]^+$ and $[\text{Cp}^*(\text{PMe}_3)\text{Ir}(\text{Ph})(\text{CO})]^+$ while liberating C_2H_4 and CH_4 . During competition experiments between these two aldehydes for 6 in the bulk reaction mixture, no selectivity was observed and both reaction products were formed in a 1:1 ratio. Remarkably, the host–guest

complex 7 is able to distinguish between these two substrates on the basis of their size, resulting in an exclusive reaction with acetaldehyde (Scheme 4b). This reaction is likely to be initiated via substitution of the coordinating C_2H_4 for the aldehyde (Scheme 4c). Afterward, metal insertion into the aldehyde C–H bond occurs, resulting in an iridium acyl intermediate. A migratory deinsertion follows, resulting in the formation of the carbonyl complexes $[\text{Cp}^*(\text{PMe}_3)\text{Ir}(\text{R})(\text{CO})]^+$ and liberation of methane. Notably, as cage 5 and the encapsulated carbonyl complexes $[\text{Cp}^*(\text{PMe}_3)\text{Ir}(\text{R})(\text{CO})]^+$ are both chiral, two diastereomeric host–guest assemblies are the potential products. For acetaldehyde, a diastereomeric ratio (dr) of 60:40 has been reported. In addition to the size of the substrate, the substrate shape also has an impact on the reaction outcome. 7 reacts with a different diastereoselectivity with the two aldehydes butyraldehyde and isobutyraldehyde. The product of the reaction with butyraldehyde is obtained with a dr of 70:30, while the reaction product with isobutyraldehyde shows only a poor diastereoselectivity of 55:45.

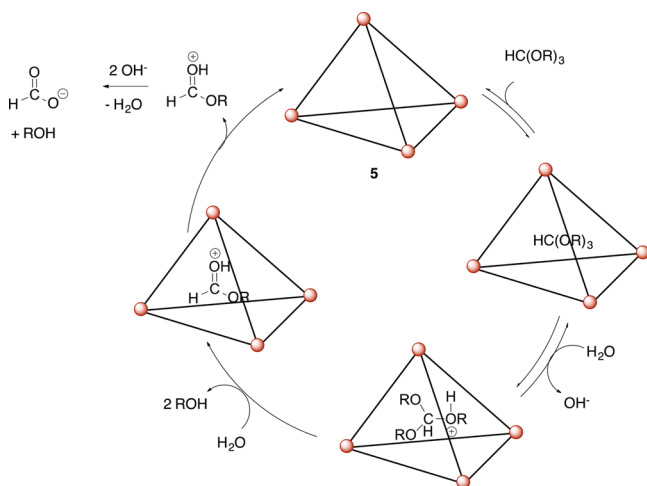
Bergman and Raymond showed later that encapsulation of $[\text{Cp}^*(\text{PMe}_3)\text{Ir}(\text{Me})(\text{cis-2-butene})]^+$ (8) in the Ga_4L_6 cage 5 results in the formation of host–guest complex 9.³² Similar to the case for 7, 9 can activate C–H bonds of aldehydes. In addition, the ability of 9 to activate C–H bonds in ethers was demonstrated (Scheme 5a). The products of these transformations are Fischer-type carbene complexes. The reaction starts with a substitution of the olefin for the ether substrate (Scheme 5b). Afterward the C–H bond activation of the carbon in a position α to the ethereal oxygen occurs. After loss of methane, an α -hydride elimination occurs. This results in the formation of the Fischer-type carbene complex. Interestingly, 9 reacts exclusively with small ether compounds. Examples are dimethyl ether (Me_2O) and ethyl methyl ether (EtOMe). Larger substrates, such as methyl *n*-propyl ether (MeOPr), diethyl ether (Et_2O), and tetrahydrofuran (THF) do not react with 9, although free 8 reacts readily in the absence of the Ga_4L_6 cage 5 with those substrates. The Fischer-type carbene complexes are chiral at the metal center. Similar to the case described above (Scheme 4), the chiral cage 5 and the chiral encapsulated carbene complex result in a mixture of diastereomers. For the reaction with Me_2O a diastereomeric ratio of 88:12 was observed. Interestingly, heating the encapsulated Fischer-type carbene complexes for several hours at 75 °C resulted in a decrease of the dr to 58:42.

Scheme 5. (a) Size-Selective C–H Bond Activation of Ethers by Host–Guest Complex 9 and (b) Mechanism of the C–H Bond Activation of Ethers³²



In addition to these stoichiometric transformations, Bergman and Raymond also reported later catalytic size-selective transformations. In 2007 they demonstrated that molecular flask **5** can be used to perform acid-catalyzed orthoformate hydrolysis in a basic solution (Scheme 6).³³ The catalyst **5** is

Scheme 6. Mechanism of the Orthoformate Hydrolysis Catalyzed by **5**³³



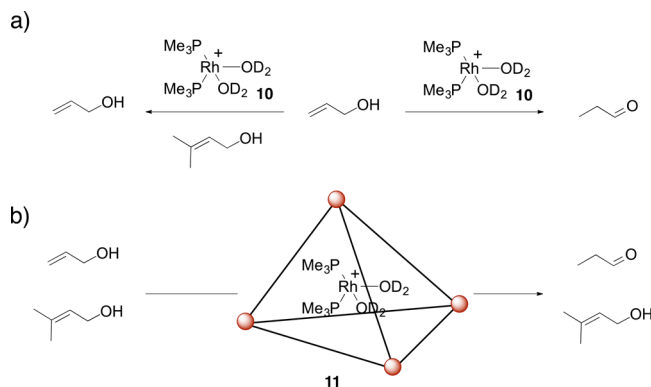
soluble in aqueous basic solutions and offers a hydrophobic interior favoring the formation of a neutral host–guest complex with orthoformates. After the encapsulated orthoformate is protonated from water, two successive hydrolysis steps occur inside the cavity, liberating 2 equiv of alcohol. Afterward, the protonated formate ester compound leaves cage **5** to become deprotonated and hydrolyzed in the basic bulk reaction mixture, resulting in the formation of the formate and the third equivalent of alcohol. As a result of the confined space, only substrates with alkyl ether groups smaller than pentyl could be hydrolyzed.

A kinetic analysis of the **5**-catalyzed orthoformate hydrolysis revealed that **5** causes substantial rate acceleration over the background hydrolysis reaction under the same reaction conditions. The hydrolyses of triethyl orthoformate and triisopropyl orthoformate are 560 and 890 times faster in the presence of **5**, respectively, in comparison to the reaction in the absence of **5**. Interestingly, adding NEt_4^+ shuts down the reaction. This happens because NEt_4^+ is a strongly binding guest that inhibits binding of the substrate to **5**.

Moreover, **5** has also been shown to encapsulate rhodium complexes such as $[(\text{PMe}_3)_2\text{Rh}(\text{OD}_2)_2]^+$ (**10**), resulting in host–guest complex **11**.³⁴ Free **10** isomerizes a broad scope of allyl alcohols and allyl ethers in the bulk reaction mixture. However, in the presence of crotyl alcohol the reactivity of **10** is shut down, resulting in catalyst inhibition and no further conversion of other reactants such as allyl alcohol (Scheme 7a). Strikingly, when **11** was used as the catalyst, substantial size selectivity was observed (Scheme 7b). Allyl alcohol in the presence of 10 mol % of **11** is isomerized within 30 min to propionaldehyde (95% yield). Interestingly, **11** is also able to isomerize allyl alcohol even in the presence of crotyl alcohol, which is not possible with **10**. This example demonstrates the ability of cage compounds to protect their reactive sites from deactivation through reagents that are located in the bulk reaction mixture.

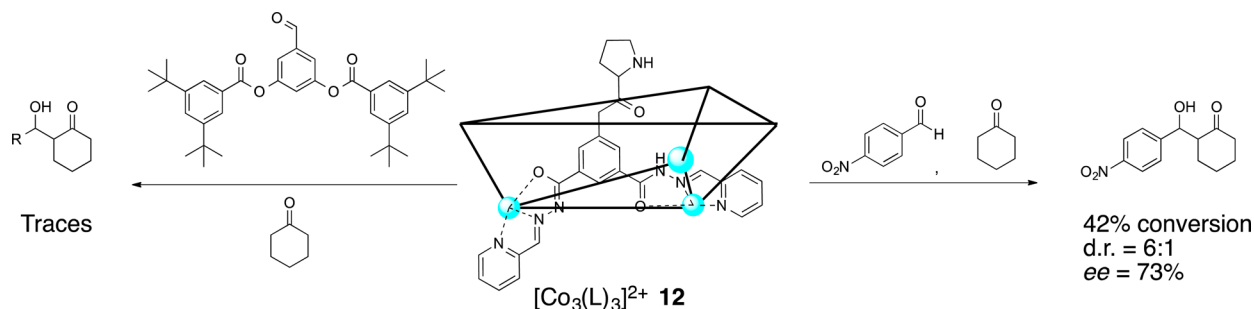
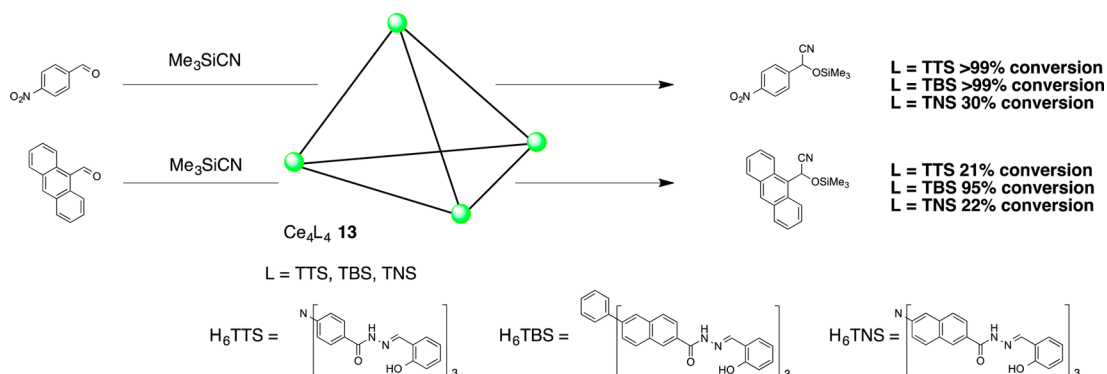
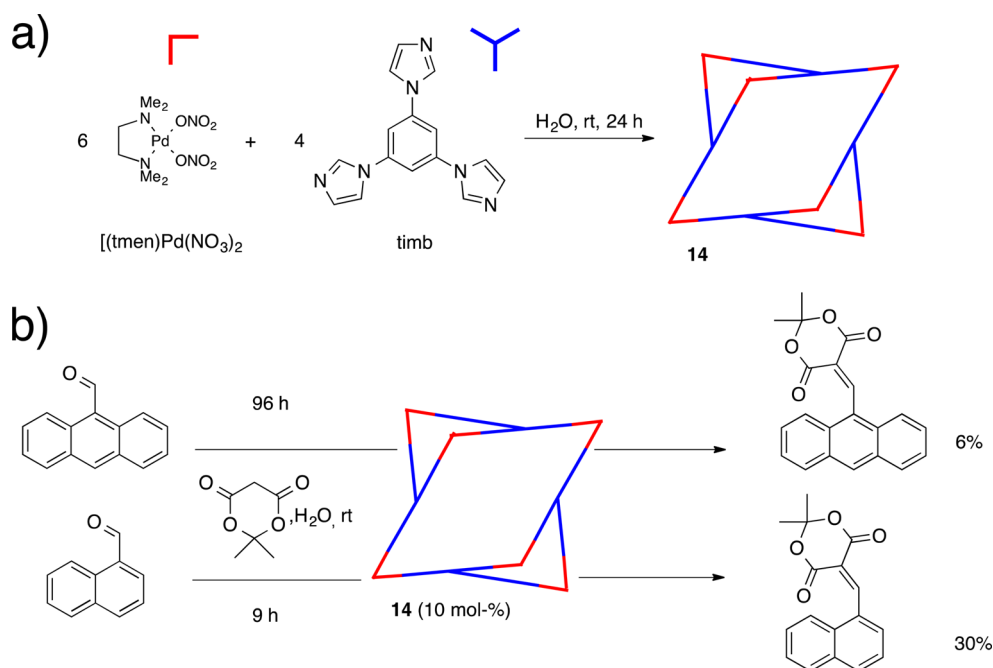
Duan and co-workers reported in 2011 the synthesis of the triangle-shaped M_3L_3 cavity **12** that assembles via coordination

Scheme 7. (a) Effect of the Presence and Absence of Crotyl Alcohol for the **10-Catalyzed Isomerization of Allyl Alcohol to Propionaldehyde and (b) Size-Selective Isomerization of Allyl Alcohol to Propionaldehyde in the Presence of Crotyl Alcohol Catalyzed by **11****³⁴



to cobalt (Scheme 8).³⁵ The ligand has additional *L*-proline moieties attached to its backbone. Due to this functionalization **12** has an enantiomerically enriched helical-like cavity. The *L*-proline units are catalytically active sites for asymmetric aldol reactions. For the aldol reaction with cyclohexanone, 42% of 4-nitrobenzaldehyde was converted in the presence of 1.5 mol % of **12**. The aldol product was formed with a diastereoselectivity of 6:1 (anti:syn), and an ee of 73% was reported. Notably, a similar coordination sphere that lacks *L*-proline functionalization gave after 10 days only trace amounts of aldol product. In the absence of cobalt ions, the ligand caused only 36% conversion of substrate. In addition, a lower diastereo- (2:1) and enantioselectivity (50% ee) were observed. The reactions catalyzed by **12** are not only enantioselective but also size selective (Scheme 8). While 42% of 4-nitrobenzaldehyde was converted by **12**, no reaction occurred when 3-formyl-1-phenylene(3,5-di-*tert*-butylbenzoate) was used as the aldehyde compound. The authors believe that this is due to the fact that this substrate is larger than the pocket size of **12**. Remarkably, when the free ligand was used, 24% of 3-formyl-1-phenylene(3,5-di-*tert*-butylbenzoate) was converted.

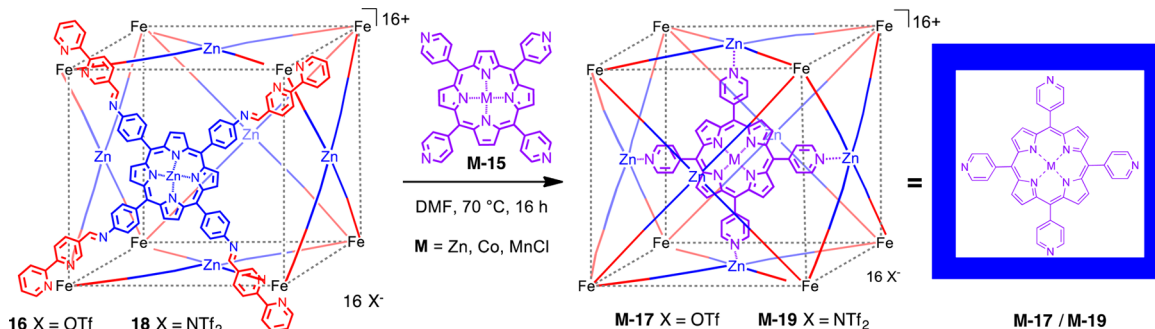
Later, the formation of the cerium-based tetrahedral molecular flask Ce_4TTS_4 (**13-TTS**, $\text{H}_6\text{L} = \text{N},\text{N}',\text{N}''$ -nitrilotris-4,4',4''-(2-hydroxybenzylidene)benzohydrazide = H_6TTS) and related compounds were reported by Duan and co-workers.^{36,37} Due to its amide-functionalized interior, **13-TTS** can interact with encapsulated guests, resulting in the ability of **13-TTS** to act as a molecular flask for the catalytic cyanosilylation of aromatic aldehydes (Scheme 9).³⁷ Several aldehydes have been tested, revealing that smaller aldehydes, such as 4-nitrobenzaldehyde, gave higher yields in comparison to aldehydes with larger substituents such as 2-(anthracen-9-yl)acetaldehyde. Substitution of the TTS ligand for the larger TBS ligand ($\text{H}_6\text{TBS} = 1,3,5$ -phenyl-4,4',4''-tris(2-hydroxybenzylidene)benzohydrazide) resulted in the assembly of the cage Ce_4TBS_4 (**13-TBS**) that offers larger pores and a larger cavity. While **13-TTS** has a pore diameter of 9.21 Å, the larger **13-TBS** offers a pore diameter of 10.24 Å. The larger pore diameter of **13-TBS** resulted in an increased substrate scope, allowing also larger compounds such as 2-(anthracen-9-yl)acetaldehyde to be substrates for the cyanosilylation. When **13-TNS** ($\text{H}_6\text{TNS} = \text{N}',\text{N}'',\text{N}'''$ -nitrilo-6,6',6''-tris(2-hydroxybenzylidene)-2-naphthohydrazide), which has a smaller pore diameter of 7.74 Å, was used as the catalyst,

Scheme 8. Size-Selective Asymmetric Aldol Reactions Catalyzed by **12**³⁵Scheme 9. Size-Selective Cyanosilylation of Aldehydes Catalyzed by **13**³⁷Scheme 10. (a) Synthesis of Molecular Flask **14** and (b) Size-Selective Knoevenagel Condensation Catalyzed by **14**³⁹

the conversion of 4-nitrobenzaldehyde decreased to 30%, while similarly to **13-TTS**, 22% of 2-(anthracen-9-yl)acetaldehyde was converted. The three catalysts **13-TTS**, **13-TBS**, and **13-TNS** are good examples of how the reactivity and selectivity of a molecular flask can be fine-tuned via control of the pore size.

Fujita and co-workers reported in 2012 on a 12+ charged Pd_6L_4 ($\text{Pd} = \text{Pd}(\text{NH}_2\text{CH}_2\text{CH}_2\text{NH}_2)$ and $\text{L} = 2,4,6\text{-tris}(4\text{-pyridyl})\text{-}1,3,5\text{-triazine}$; NO_3^- as counterion) cationic coordination cage

that is able to catalyze the Knoevenagel condensation of aromatic aldehydes and Meldrum's acid.³⁸ The reactions occur under neutral conditions using water as the reaction solvent. As control experiments show, the cage catalyst has a dramatic impact on the reaction outcome. For instance, while 2-(anthracen-9-yl)acetaldehyde shows close to no reactivity in the absence of the cage (yield <1%), the corresponding Knoevenagel condensation product was obtained in 63% yield when the reaction was performed under the same conditions but in

Scheme 11. Encapsulation of M-15 in 16/18 To Give Host–Guest Complexes M-17/M-19^{a,20,42,43}

^aReproduced from ref 43. Copyright 2016 American Chemical Society.

the presence of the Pd₆L₄ cage. The authors propose a mechanism that involves encapsulation of the aromatic aldehyde. Meldrum's acid is deprotonated outside the cage, resulting in the formation of the corresponding enolate. The enolate attacks the encapsulated aldehyde, resulting in the formation of an oxyanion intermediate inside the cationic cage. They propose that the cage facilitates the Knoevenagel condensation, as the cationic charge of the cage is able to stabilize this anionic intermediate.

Mukherjee and co-workers reported later in 2012 on the assembly of the Pd₆L₄ coordination cage **14** from 4 equiv of 1,3,5-tris(1-imidazolyl)benzene (timb) and 6 equiv of [(tmen)-Pd(NO₃)₂]₂ (tmen = N,N,N',N'-tetramethylethylenediamine) (Scheme 10a).³⁹ They demonstrated that this system is able to catalyze Knoevenagel condensation reactions of aromatic aldehydes with Meldrum's acid and 1,3-dimethylbarbituric acid. Similarly to the work reported by Fujita and co-workers, the cage **14** has a clear effect on enhancing the reaction rate of the Knoevenagel condensation. This effect is prominent in particular for larger aromatic aldehydes such as pyrene-1-aldehyde and 2-(anthracen-9-yl)acetaldehyde. Notably, smaller aldehydes such as 1-naphthaldehyde give in general higher yields and are converted more quickly. While 2-(anthracen-9-yl)acetaldehyde gives with Meldrum's acid and 10 mol % of catalyst after 96 h only 6% Knoevenagel condensation product, 1-naphthaldehyde is obtained in a yield of 30% after only 9 h (Scheme 10b). Notably, a blank experiment in the absence of the cage gives 15% of the 1-naphthaldehyde condensation product, suggesting that both the cage effect and conversion in the bulk reaction mixture contribute to the higher observed yield. In addition, **14** is also able to catalyze Diels–Alder reactions. More recently, Mukherjee and co-workers reported on an additional molecular flask to catalyze Knoevenagel condensations. They described a Pd₇L₂L'₂ cage that assembles via a rare social self-sorting phenomena of 2 equiv of the ligands timb and tim (1,2,4,5-tetrakis(1-imidazolyl)benzene) and [(tmen)Pd(NO₃)₂]₂.⁴⁰

de Bruin and co-workers reported in 2013 the encapsulation of zinc and cobalt tetrapyrroline-porphyrins (M-15) in the cubic Fe₈L₆ cage **16** to yield the host–guest complex M-17 (Scheme 11).²⁰ Cage **16** is a larger derivative of the Fe₈L₆ cage previously reported by Nitschke and co-workers.⁴¹ Cage **16** assembles from 6 equiv of tetrakis(4-aminophenyl)-porphyrinatozinc(II) that reacts in the presence of 8 equiv of Fe(OTf)₃ via imine condensation with 24 equiv of a 5-bipyridine-aldehyde. The iron ions are located in the corners of the cubic cage and are each chelated by three bipyridine moieties. Each bipyridine moiety is connected to a porphyrin

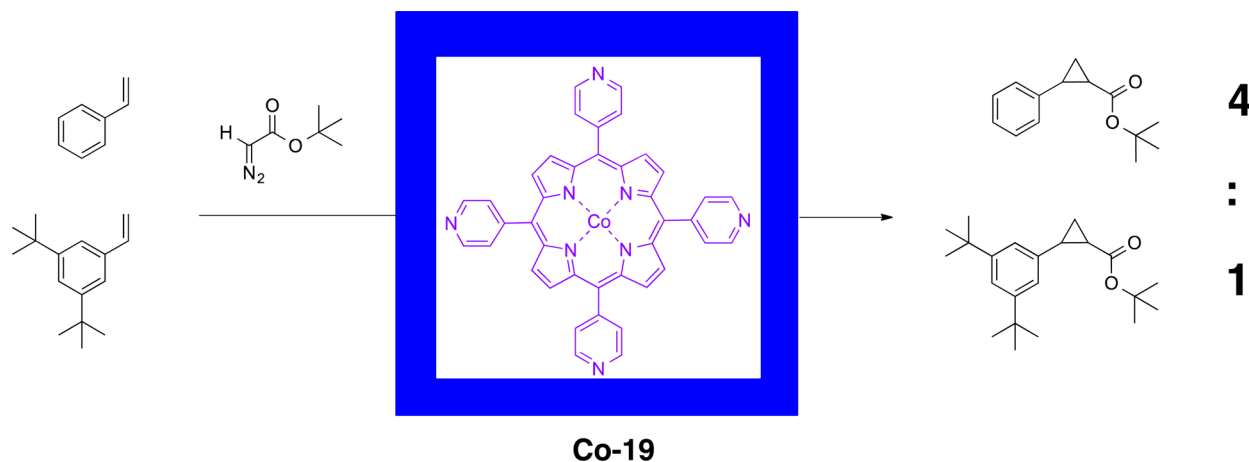
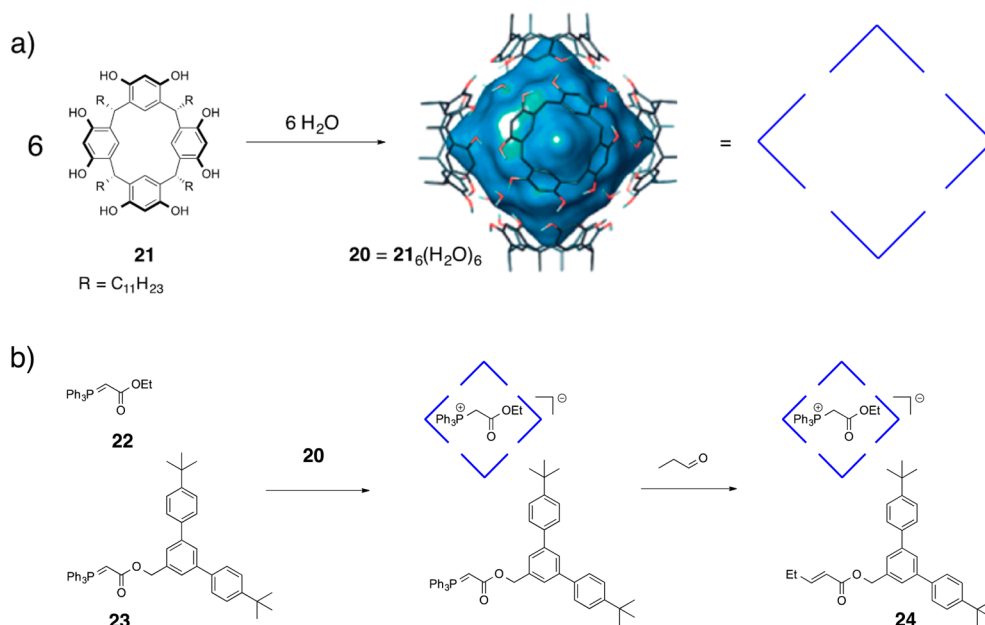
via an imine linker. The porphyrins are located on the cube faces. Similarly to the work of Nguyen and Hupp the porphyrin encapsulation of M-15 occurs via coordination of pyridine moieties to the zinc ions of the cavity.

Co-17 has been shown to activate diazo compounds, enabling reactions with alkenes to yield cyclopropanes. The reactivity of the encapsulated cobalt-porphyrin in Co-17 is significantly increased in comparison to the free Co-15. For instance, the cyclopropanation of styrene with ethyl diazoacetate by Co-15 gives only a TON of 9 (trans:cis = 67:33) after 1 h, while Co-17 has accomplished 33 turnovers (trans:cis = 65:35). It is believed that Co-15 gives a lower TON due to the intermolecular coordination of pyridine from one porphyrin to the reactive cobalt center of another porphyrin. Due to encapsulation, this blocking of the reactive site is prevented. In addition, Co-17 catalyzes a diastereoselective olefin synthesis from diazo compounds that is most likely to occur via a 1,2-hydrogen atom shift.

Later, it was shown that the cage performance could be further improved through substitution of the counterion (change from OTf⁻ to NTf₂⁻), resulting in the formation of **18**.⁴² After encapsulation of Co-15, host–guest complex Co-19 was obtained (Scheme 11). Co-19 allowed the catalytic cyclopropanation to be performed at lower temperature and lower catalyst loadings while enabling the use of a broader solvent scope (e.g., water/acetone mixtures). In addition, the use of the more easily handled *N*-tosylhydrazones as substrates for cyclopropanation reactions is possible with Co-19. Moreover, Co-19 can catalyze the cyclopropanations of a broad scope of olefins with different diazo compounds.

During these studies higher yields for the conversion of smaller substrates were observed in general. In addition, competition experiments showed that smaller substrates are the preferred reaction partners for Co-19. For instance, when a 1:1 mixture of styrene and 3,5-di-*tert*-butylstyrene reacted in the presence of Co-19 (0.25 mol %) with *tert*-butyl diazoacetate, a 4:1 size selectivity for the cyclopropanation of styrene over 3,5-di-*tert*-butylstyrene was observed (Scheme 12). Notably, cobalt tetraphenylporphyrin (Co-TPP) gave for the same substrate composition a 1:1 mixture of cyclopropanation products.

In a very recent report by de Bruin and co-workers, the encapsulation of manganese chloride tetrapyrroline-porphyrin (MnCl-15) resulted in the formation of the cage MnCl-19.⁴³ MnCl-19 has been shown to be an effective epoxidation catalyst for a broad scope of substrates. Similarly to Co-19, MnCl-19 is also able to distinguish substrates on the basis of their size. The observed size selectivity between styrene and

Scheme 12. Size-Selective Cyclopropanation of Olefins Catalyzed by Co-19⁴²Scheme 13. (a) Self-Assembly of 20^{49,50} and (b) Size-Selective Wittig Reaction Mediated by 20⁵⁰

^aReproduced from ref 50. Copyright 2013 American Chemical Society.

3,5-di-*tert*-butylstyrene is around 2:1. In comparison to the systems described by Nguyen and Hupp,²⁹ who observed up to a 7:1 ratio, the selectivity is less good. On the other hand, it is very challenging to obtain size selectivity for the conversion of monosubstituted olefins.

III. ORGANIC SUPRAMOLECULAR CAVITIES

The second frequently investigated class of cavities that are formed via self-assembly is of an organic supramolecular nature. Hydrogen-bonding motifs are here mainly, but not exclusively, found, resulting in exciting structures including “tennis balls”,⁴⁴ “softballs”,⁴⁵ and many others.^{5,46} In addition, these kinds of molecular architectures have been used as molecular flasks. Examples are their applications in Diels–Alder reactions,⁴⁷ 1,3-dipolar cycloadditions,^{19a} and photochemical transformations.⁴⁸ Similarly to cavities that result from metal–organic coordination, organic supramolecular cavities have been shown to act as size-selective molecular flasks.

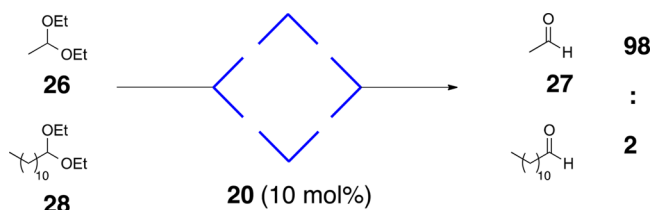
Atwood and co-workers described in 1997 the synthesis of the hexameric resorcin[4]arene capsule 20.⁴⁹ In polar solvents, 20 assembles readily from six resorcin[4]arene units 21 (Scheme 13a). Tiefenbacher and co-workers reported in 2013 that 20 is a Brønsted acid with a pK_a of 5.5–6.⁵⁰ In the same study, they showed that 20 (1.0 equiv) is able to encapsulate the stabilized Wittig ylide $\text{Ph}_3\text{P}=\text{CHCO}_2\text{Et}$ (22; 0.85 equiv). Due to the Brønsted acidity of 20, encapsulated 22 is protonated, resulting in $\text{Ph}_3\text{P}^+\text{CH}_2\text{CO}_2\text{Et}@20^-$ (Scheme 13b). As a consequence, encapsulated 22 is unreactive toward added propanal (10 equiv). This demonstrates that 20 is able to prohibit Wittig reactions due to encapsulation and protonation. Notably, when the sterically more demanding ylide ester 23 is used, encapsulation and thus protonation cannot occur. Instead, the Wittig reaction takes in the presence of propanal (1.5 equiv) in the bulk solution place and yields alkene 24 (66% after 16 h). When competition experiments of the two ylides 22 (0.85 equiv) and 23 (0.85 equiv) were performed in

the presence of **20** (1.0 equiv), **24** was isolated in 74% yield (*E*:*Z* = 14:1), while EtCH=CHCO₂Et (**25**) resulting from the reaction of **22** with propanal has only been observed in traces (3%, Scheme 13b). Interestingly, without **20** but under otherwise identical reaction conditions a 47:53 mixture of **24** and **25** was obtained.

Although **20** was used in stoichiometric amounts, the size selectivity observed here is very interesting. The cavity was used here to prevent the smaller substrate **22** from participating in the reaction while the large substrate **23** was converted. This is a remarkable difference from most other reported size-selective transformations that are mediated or catalyzed by molecular flasks, as those support in general the conversion of the smaller substrate.

In addition to the ability to mediate size-selective Wittig reactions, Tiefenbacher and co-workers reported in the same work that Brønsted acid **20** is also able to catalyze the size-selective hydrolysis of diethyl acetals in water-saturated CDCl₃ at 25 °C (Scheme 14). Here, the smaller substrate 1,1-diethoxyethane

Scheme 14. Size-Selective Hydrolysis of Diethyl Acetals Catalyzed by **20**⁵⁰



(**26**) was selectively converted into the corresponding aldehyde **27**, while the larger diethyl acetal 1,1-diethoxydodecane **28** reacted poorly. A competition experiment between **26** and **28** in the presence of **20** (10 mol %) revealed after 60 min 85% combined conversion and a 98:2 preference for the formation of acetaldehyde over dodecanal. When catalyst **20** was replaced for 400 mol % TfOH, 24% acetaldehyde and 41% dodecanal (ratio of 37:63) were obtained after 1 h. Notably, the catalytic activity of **20** can be shut down due to encapsulation of a strongly binding inhibitor such as Bu₄N⁺, resulting in only a weak background reaction.

In a more recent study, the authors reported that **20** is also able to catalyze terpene cyclizations that occur inside its cavity.⁵¹ In addition, **20** can also catalyze the hydroalkoxylation of unsaturated alcohols.⁵² Although a broad scope of substrates has been shown to undergo this transformation, size selectivity was observed during competition experiments between **29** and the more bulky derivative **30** (Scheme 15). The corresponding cyclization products **31** and **32** were obtained after 64 h in a 92:8 ratio, favoring the tetrahydropyran **31** that stems from the

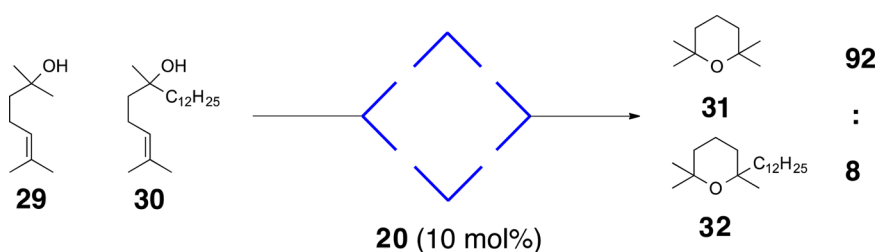
sterically less demanding alcohol **29**. When capsule **20** was replaced by 10 mol % TfOH, products **31** and **32** were obtained in a ratio of 46:54.

The groups of Strukul and Scarso also studied the use of **20** as a catalyst. In 2011 they showed, in cooperation with the group of Reek, that **20** can encapsulate an Au(NHC) complex, resulting in new chemo- and regioselectivities for the conversion of a terminal alkyne.^{16c} Strukul and Scarso and co-workers showed more recently that **20** can also catalyze the conversion of isonitrile substrates into *N*-formylamides.⁵³

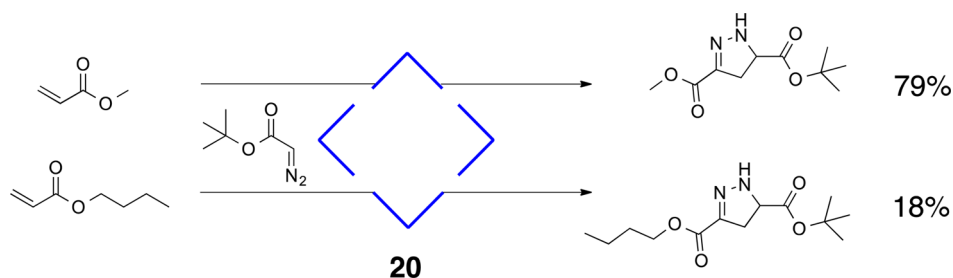
In addition to that report, they were able to demonstrate further application of **20** in size-selective catalysis in 2015. It has been shown that **20** is capable of catalyzing the 1,3-dipolar cycloaddition reaction between diazoacetate esters and electron-poor alkenes.⁵⁴ The yields observed for these transformations differ significantly from those obtained in the absence of **20**. For instance, when *tert*-butyl diazoacetate and acrolein were reacted in the presence of **20**, 97% of the 1,3-dipolar cycloaddition product was obtained, while only 25% was obtained in the absence of **20**. Similarly to catalytic results reported by Tiefenbacher and co-workers,^{50,52} the catalytic ability of **20** can be shut down through addition of ammonium salts, as in comparison to the substrates they have a stronger binding tendency to **20**. When *tert*-butyl diazoacetate was reacted with different acrylate esters, **20** showed a preference for ester compounds with shorter alkyl chains (Scheme 16). For instance, while the reaction with the methyl ester gave 79% yield, only 18% of desired product was obtained when the *n*-butyl ester was used.

In addition, carbodiimides form host–guest complexes with **20** (Scheme 17). The cavity offers sufficient space to even coencapsulate additional carboxylic acids and amines, allowing the synthesis of amides. Due to the restricted space inside the cavity, amides with smaller substituents are preferred during competition experiments (Scheme 17).⁵⁵ These experiments were carried out between two carboxylic acids (hexanoic and dodecanoic acid) and two amines (butylamine and octylamine). Out of four possible products, *N*-butylhexanamide, which results from the reaction of hexanoic acid and butylamine, is the smallest. With a yield of 50%, *N*-butylhexanamide has been shown to be the major product in the presence of **20**. The two large amides that result from the reaction with dodecanoic acid have been obtained in low yields of between 4 and 6%. Remarkably, in the absence of **20** the amide synthesis was much less selective and all four possible products have been obtained in yields between 12 and 28%. It has to be noted that the example from Scheme 17 is different from most other size-selective molecular flasks described. Cage **20** has shown to be able to size selectively form one out of four potential products while in most other examples size exclusion occurs only between two different substrates.

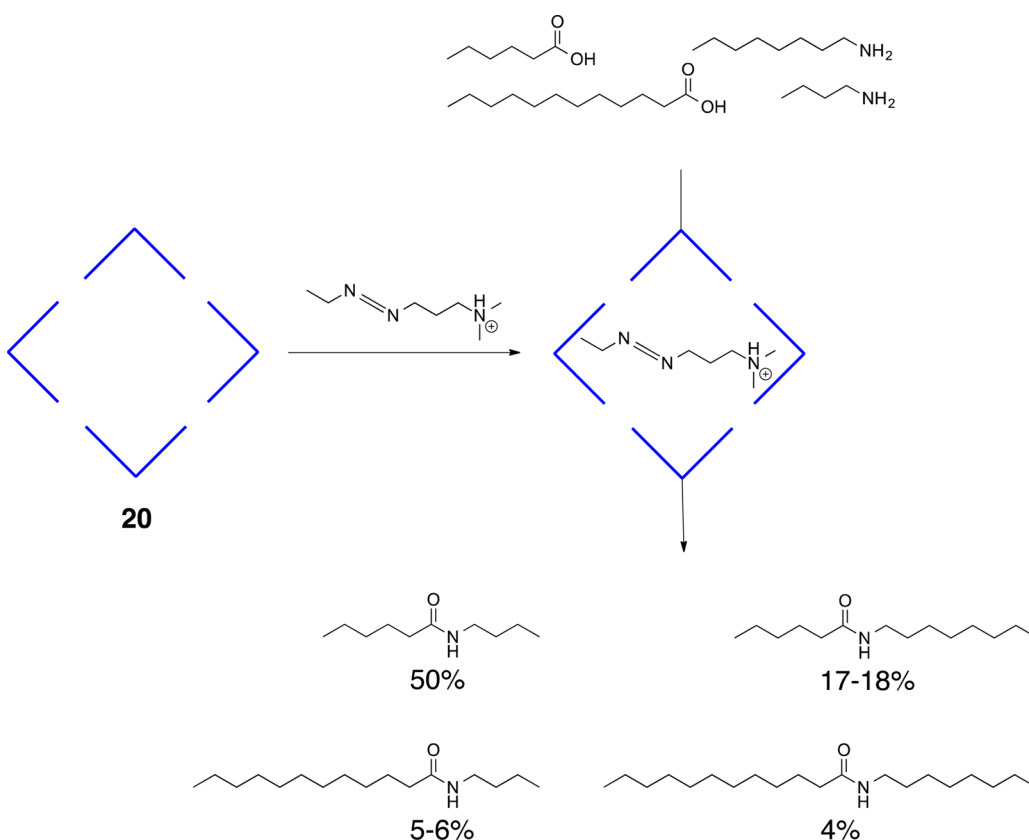
Scheme 15. Size-Selective Hydroalkoxylation of Unsaturated Alcohols Catalyzed by **20**⁵²



Scheme 16. Size-Selective 1,3-Dipolar Cycloaddition between *tert*-Butyl Diazoacetate and Electron-Poor Alkenes Catalyzed by **20**⁵⁴



Scheme 17. Size-Selective Amide Synthesis Catalyzed by **20**⁵⁵



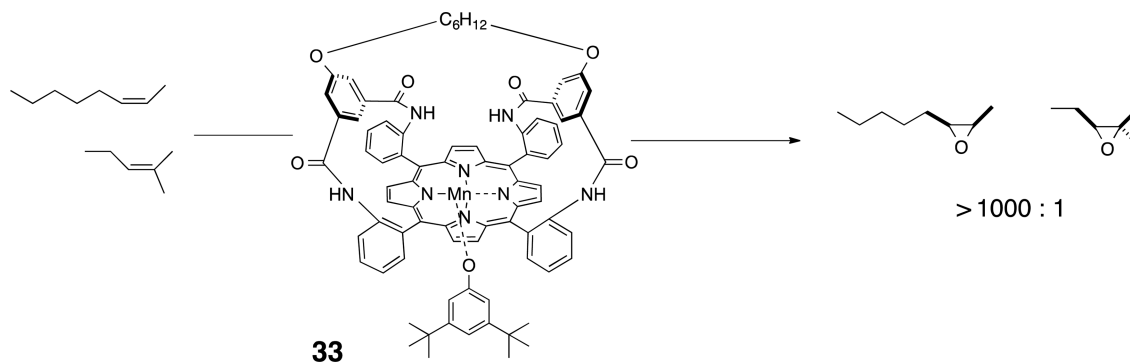
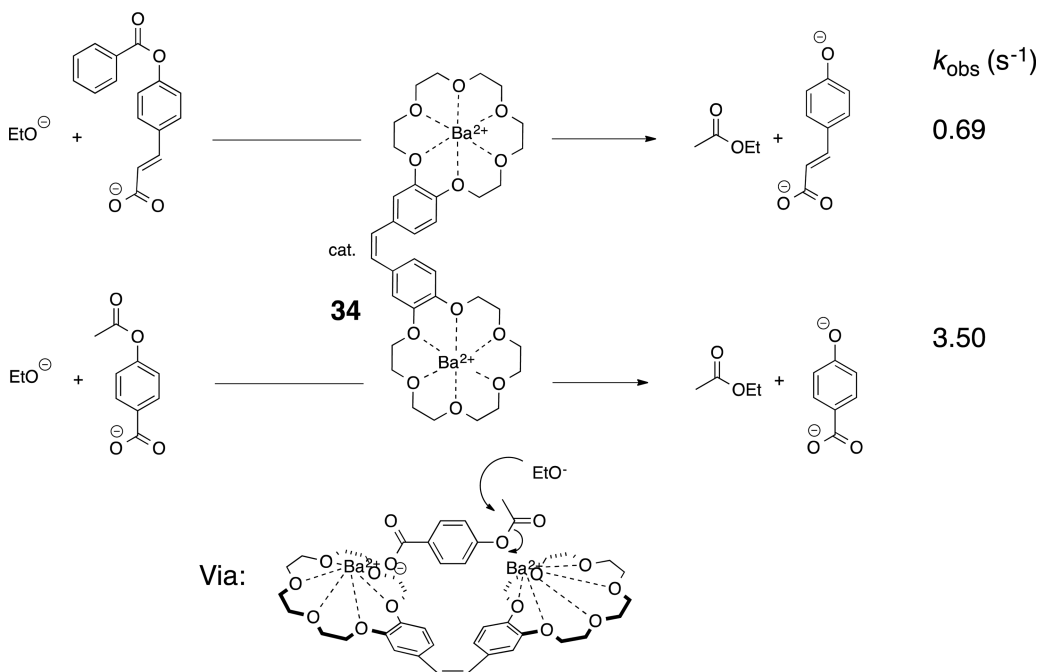
IV. ORGANIC COVALENT CAVITIES

The development of cavities that are of a purely organic nature and do not assemble via supramolecular interactions such as metal–ligand coordination or hydrogen-bonding phenomena has a different history. Those covalent architectures used to be synthesized via irreversible kinetically controlled reactions, which gave the desired reaction products typically in low yields. The reason is that undesired oligomerization often competes with the desired ring- or cage-closing bond formation. Once an undesired bond has been formed, it cannot be repaired. This results often in complicated product mixtures that are difficult to purify. This is a major difference from the cavities that are obtained from metal–ligand coordination or other supramolecular interactions, as those are able to undergo self-healing processes. In this regard, cavity design via supramolecular interaction has been established for most cases as the preferred method.

Within recent years, the synthesis of purely organic and covalent cavities has more often been accomplished by employing reactions that occur under thermodynamic control. In contrast

to classic kinetically controlled approaches, cavity synthesis via so-called dynamic combinatorial chemistry (DCC) allows self-healing processes. This means that bond-forming reactions are reversible, often resulting in higher yields of the desired products. DCC became of great interest in recent years and resulted in the development of many new cavities.⁵⁶ However, reports on molecular flasks that have been synthesized via DCC are still rare in comparison to other cavity types.⁵⁷ Most reported examples of size-selective purely organic covalent molecular flasks are based on cavities that are obtained via kinetically controlled reactions. In this regard, with comparison to the previous sections, the examples discussed here (section IV) are often less recent.

Suslick and co-workers reported in 1986 on the use of manganese and iron porphyrins with sterically protected pockets as catalysts for alkane hydroxylation.⁵⁸ It was shown that a given substrate could be transformed in a shape-selective manner. Using Mn(TTPPP(OAc)) ((5,10,15,20-tetrakis(2',4',6'-triphenylphenyl)porphyrinato)manganese(III) acetate) as the catalyst

Scheme 18. 33-Catalyzed Epoxidation of Alkenes⁵⁹Scheme 19. Size-Selective Ester Ethanolysis Catalyzed by **34**⁶⁰

and iodosylbenzene as the oxidant, the hydroxylation of 2,2-dimethylbutane occurred selectively on the least hindered primary carbon (4-position), giving 3,3-dimethylbutan-1-ol as the major product over 2,2-dimethylbutan-1-ol and 3,3-dimethylbutan-2-ol (ratio ~70:5:25). Notably, this selectivity was slightly lower when Fe(TPPPP(OAc)) was used. When Mn-TPP (TPP = tetraphenyl-porphyrin), which has a more easily accessible reactive site, was used, selective oxidation on the secondary carbon occurred, giving 3,3-dimethylbutan-1-ol, 2,2-dimethylbutan-1-ol, and 3,3-dimethylbutan-2-ol in a ratio of ca. 1:9:90.

Four years later Collman and co-workers described the use of manganese picnic basket porphyrins for the epoxidation of alkenes (Scheme 18).⁵⁹ The reactions were carried out in dry acetonitrile using iodosylbenzene as the oxidation reagent. In order to observe selectivity effects occurring from the picnic basket site of the catalyst, the open site had to be blocked with 3,5-di-*tert*-butylphenoxide as a bulky anionic axial ligand that would not be oxidized during catalysis. Indeed, catalyst **33** is able to distinguish between different olefins on the basis of their substitution patterns. For example, the 1,2-disubstituted alkene (*Z*)-oct-2-ene is converted with a selectivity of over 1000:1 in comparison to the trisubstituted alkene 2-methylpent-2-ene

(Scheme 18). In a typical reaction protocol 125 equiv of each olefin was stirred at room temperature in acetonitrile in the presence of 55 equiv of iodosylbenzene and 1 equiv of catalyst **33**. Mn-TPP catalyzes the reaction under identical conditions with close to no selectivity.

Cacciapaglia and Mandolini and co-workers reported in 2002 on the size-selective cleavage of carboxylate-functionalized esters and anilides.⁶⁰ These reactions have been catalyzed by dinuclear barium(II) complex **34** (Scheme 19). The barium centers in **34** are each complexed by an 18-crown-6 moiety and are connected via a *cis*-stilbene linker. This complex enhances the reaction rates dramatically in comparison to single barium(II) 18-crown-6 complexes. For instance, the **34**-catalyzed conversion of 4-acetoxybenzoate is 107 times faster in comparison to its conversion catalyzed by twice the amount of the corresponding single barium(II) 18-crown-6 complex. The two metal ions in complex **34** act in a synergistic manner, as they form a catalyst–substrate complex that binds on two sites to the substrates. One metal center binds to the anchoring carboxylate, while the other activates the ester for ethanolysis. This binding happens to be very selectively based on the substrate size, resulting in a faster conversion of substrates of the right size. An example is shown in Scheme 19. Here the

smaller 4-acetoxybenzoate is converted 5 times faster than the larger (*E*)-3-(4(benzoyloxy)phenyl)acrylate.

In a further study the authors reported in cooperation with Reinhoudt and Ungaro and co-workers on calix[4]arene-based zinc complexes.⁶¹ The zinc ions are coordinated by tridentate *N,N,N* ligands that are connected to the calix[4]arene backbone via covalent bonds. Esters with anchoring carboxylate groups have been used as substrates to study their zinc-catalyzed methanolysis. In particular, three different calix[4]arene-based complexes have been tested. Those have either two or three zinc sites. The two complexes with two zinc sites are either 1,2-vicinal-functionalized or 1,3-functionalized. Interestingly, the trinuclear zinc complex 35 (Figure 1) has shown great selectivity

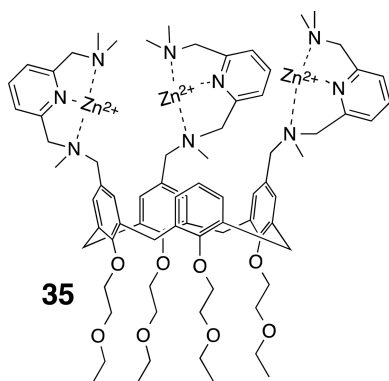


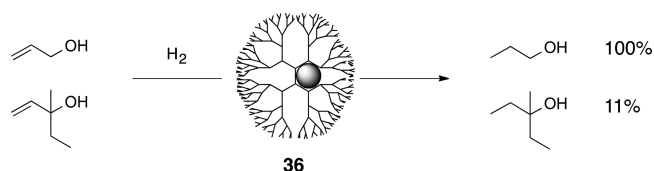
Figure 1. Size-selective ester methanolysis catalyst 35.⁶¹

for the methanolysis of ester of the right size and shape. 35 is thereby 5–6 times faster than the previously reported 34. In addition, for the regioisomeric dinuclear catalysts a striking difference in reactivity has been reported. The 1,2-vicinal-functionalized catalyst is up to 26 times more reactive in comparison to its 1,3-functionalized isomer. The comparison of the 1,2-vicinal-functionalized catalyst and 35 is less clear. Four substrates have been tested, revealing that 35 convert three of them more quickly. Thereby the difference is for the conversion of 4-acetoxybenzoate with the greatest rate enhancement of around 3.9 times.

In addition to calix[4]arenes, dendrimers have also been applied in size-selective catalysis. Crooks and co-workers reported in 2001 on dendrimers that are suitable hosts for palladium nanoparticles.⁶² Interiors of three different generations of hydroxyl-terminated poly(amidoamine) (PAMAM) dendrimers have been investigated. Those systems were tested for their abilities to act as olefin hydrogenation catalysts. Higher generation dendrimers resulted in general in a lower turnover frequency (TOF), as it is more difficult for substrates to reach the encapsulated reactive sites and to leave the host after the transformation again. For example, the TOF for the hydrogenation of but-3-en-2-ol decreased from 450 to 380 to 93, when switching from a fourth- to a sixth- to an eighth-generation dendrimer.

The steric hindrance of the described dendrimeric systems allows for their use as size-selective hydrogenation catalysts (Scheme 20).⁶³ Competition experiments between allyl alcohol and 3-methyl-1-penten-3-ol were performed in 4/1 methanol/water mixtures under atmospheric hydrogen pressure and at room temperature. In the presence of dendrimer G4OH/Pd(0)40 (36; G4 = fourth-generation dendrimer; Pd(0)40 = average of 40 Pd atoms within the dendrimer interior), a clear

Scheme 20. Size-Selective Hydrogenation of Allyl Alcohol Catalyzed by 36⁶³



size selectivity favoring the transformation of allyl alcohol was observed. While 100% allyl alcohol was converted after 5 h, only 11% of the sterically more demanding 3-methyl-1-penten-3-ol was hydrogenated. Full conversion of 3-methyl-1-penten-3-ol was observed after 42 h reaction time. Notably, outside the cavity the palladium nanoparticles act as unselective hydrogenation catalysts for olefins.

Palladium nanoparticles can also be encapsulated in other cavities. Ueno and Watanabe showed in 2004 that palladium nanoclusters encapsulated in an apo-ferrite cage can also be used as size-selective hydrogenation catalysts for olefins.⁶⁴

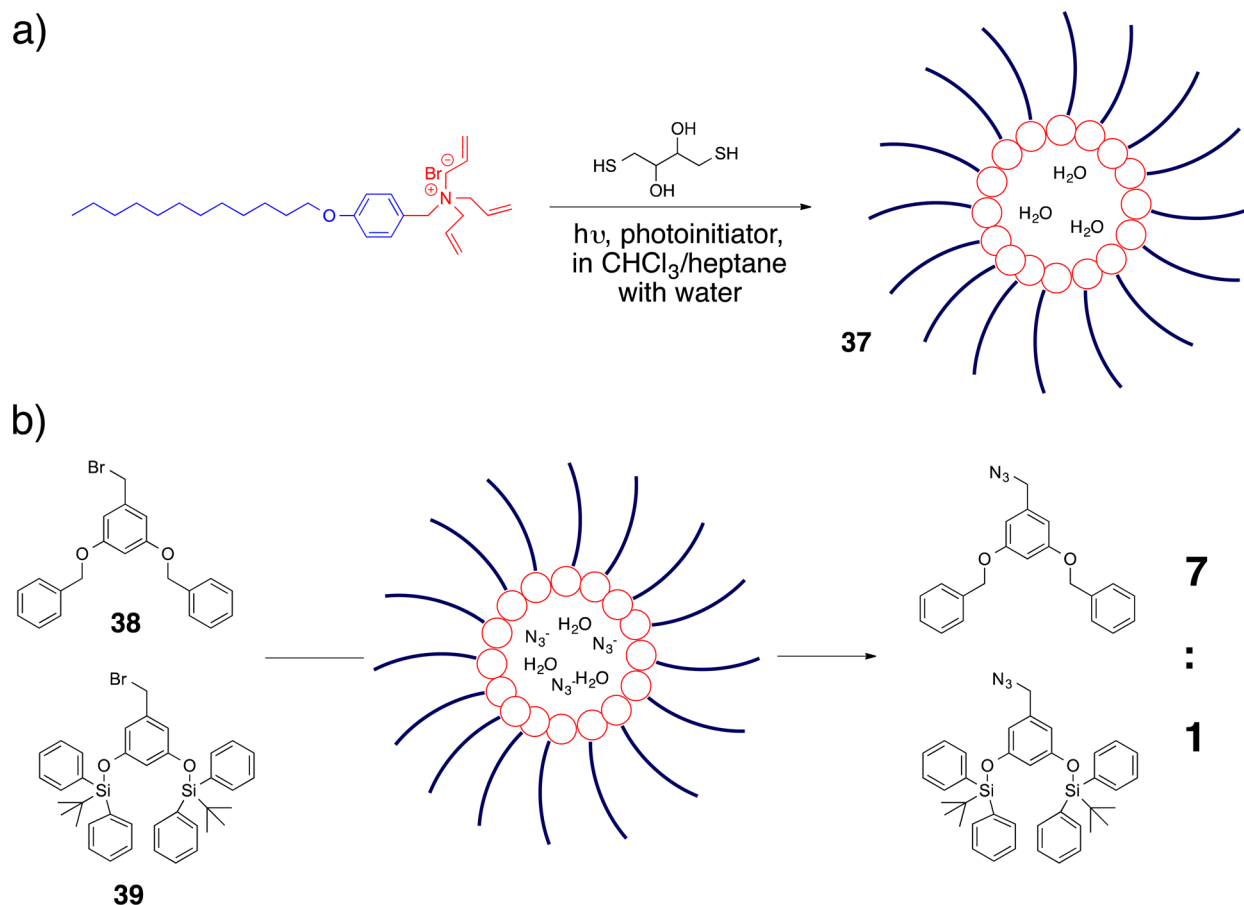
Zhao and co-workers have described another approach to size-selective molecular flasks. They reported the self-assembly of a reverse micelle made from cationic surfactants that have triallylammonium headgroups in heptane/chloroform mixtures in the presence of small amounts of water.⁶⁵ The water pool that is inside the supramolecular cavity is able to coencapsulate dithiothreitol, resulting in an efficient thiol–ene radical chain reaction, enabling the self-assembled reverse micelle to be captured by covalent bonds and resulting in the formation of 37 (Scheme 21a).

With 37 in hand, Zhao and co-workers investigated its use as a size-selective phase transfer catalyst for the nucleophilic substitution of benzyl bromides with sodium azide.⁶⁶ Sodium azide in this case is dissolved in the aqueous phase that is encapsulated by 37. Benzyl bromides of different sizes have been chosen as substrates. It has been shown that 37 has a strong effect on the reaction yields. For example, 4-bromobenzyl bromide gives the corresponding azide in the presence of 37 (20 mol %) in over 95% yield. In the absence of 37 only 8% of the product was obtained. During the course of the investigation a clear preference of 37 for converting small substrates was shown. Competition experiments between a 1:1 mixture of benzyl bromides 38 and 39 in the presence of 1 equiv of sodium azide and 37 resulted in a preference for 38 over 39 of up to 7:1 (Scheme 21b). Notably, the selectivity can be fine-tuned through controlling the size of the hydrophilic core through the amount of water used to form the reverse micelle (water:surfactant ratio). For all substrate pairs tested, the lowest size selectivity was observed for the highest water:surfactant ratio. With optimized water to surfactant ratios in hand, Zhao and co-workers have described substrate pair size selectivities of up to 9:1.

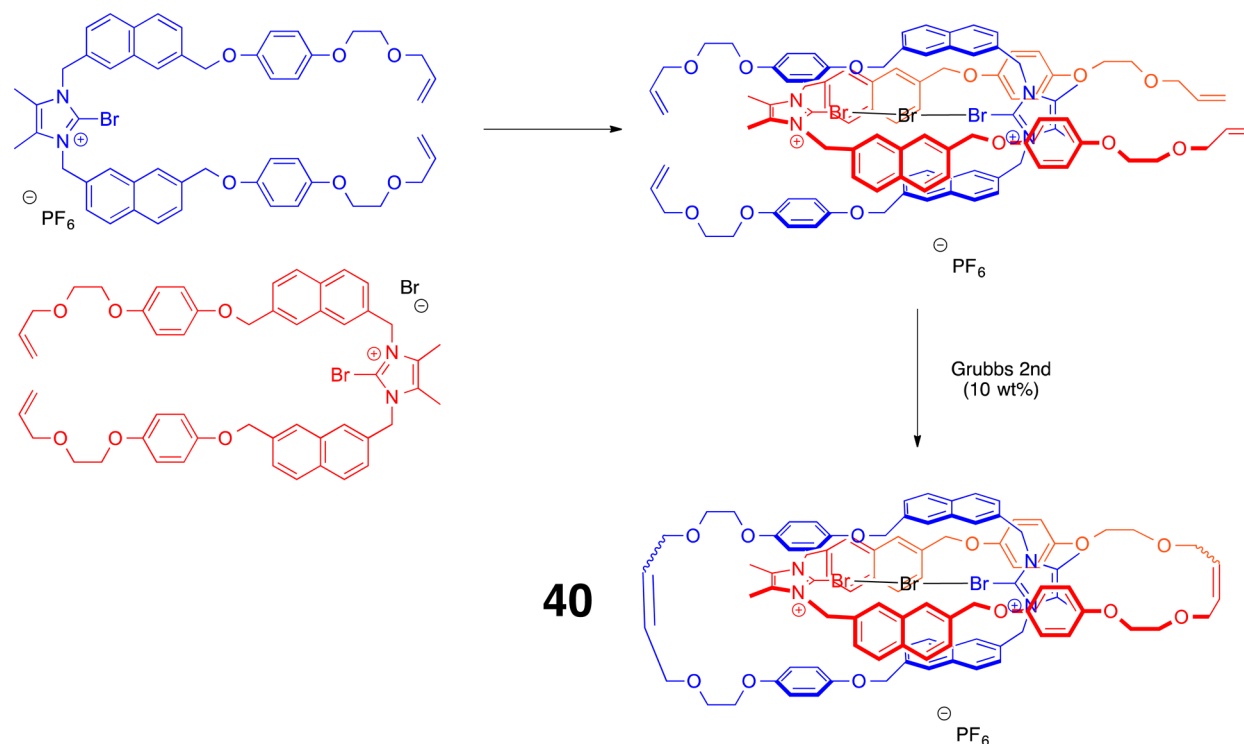
V. RECENT DEVELOPMENTS IN THE CHEMISTRY OF MOLECULAR CAVITIES

Molecular flasks have been shown to be capable of performing size-selective transformations. However, given the number of known chemical transformations, only a small percentage of those have so far been mediated or catalyzed by molecular flasks in a size-selective manner. An opportunity to increase this scope is the development of novel concepts for molecular flask design.

Scheme 21. (a) Synthesis of the Size-Selective Phase Transfer Catalyst 37 and (b) Size-Selective Azidation of 38 over 39 Catalyzed by 37⁶⁶

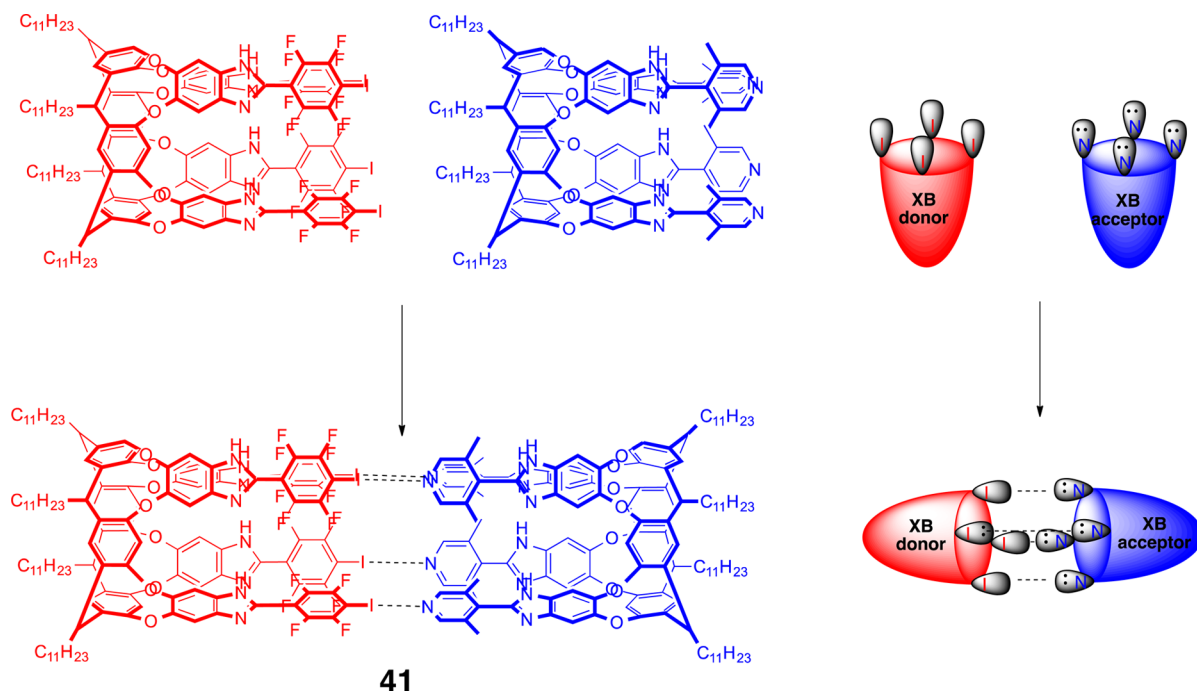
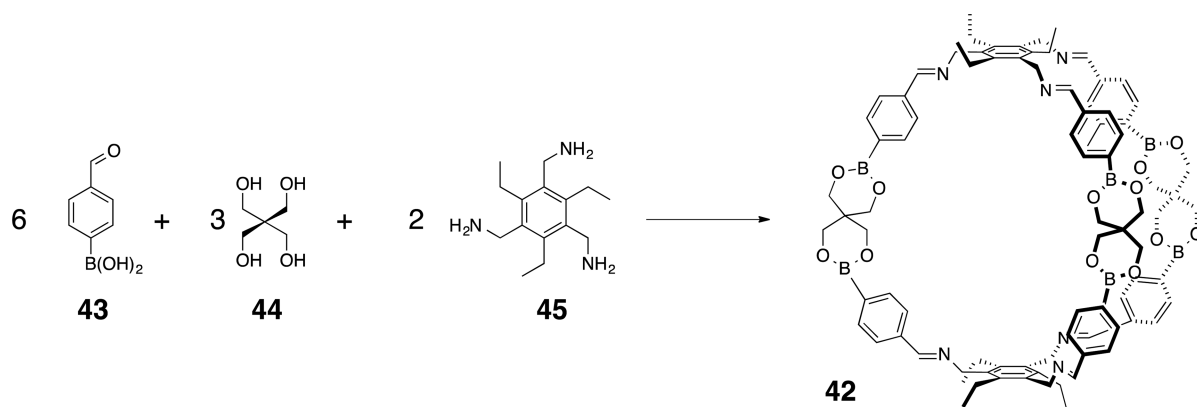


Scheme 22. Synthesis of Catenane 40 via Templating Halogen-Bonding Interaction Followed by Olefin Metathesis⁶⁷



One approach is to extend the portfolio of bonding interactions that lead to the self-assembly of molecular cavities.

Halogen-bonding interactions have recently received considerable interest. Examples are synthetic approaches to catenanes

Scheme 23. Synthesis of Cage 41 via Halogen-Bonding Interactions⁶⁹Scheme 24. Synthesis of Cage 42 via Imine Condensation and Boronic Acid–Diol Condensation⁷⁰

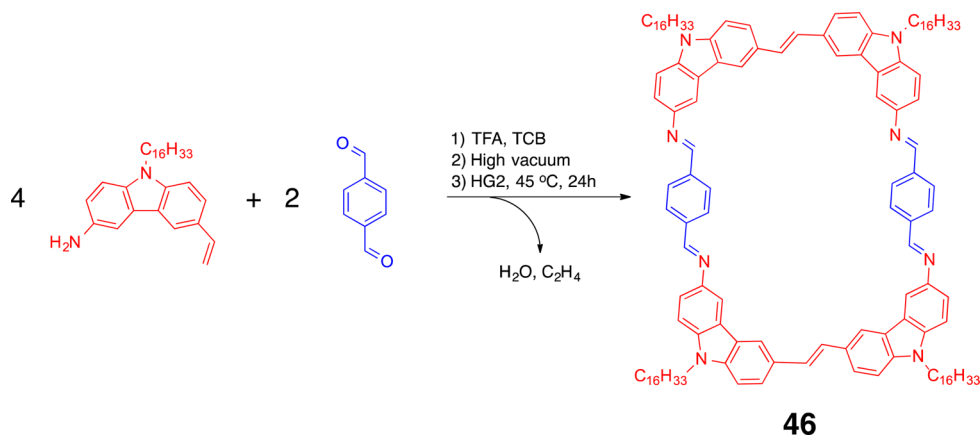
that have been reported by Beer and co-workers. They described in 2012 the synthesis of catenane **40**, which was templated by a halogen-bonding anion interaction (Scheme 22).⁶⁷ The ring closing occurred via olefin metathesis catalyzed by a Grubbs second-generation catalyst. Catenane **40** was obtained with an isolated yield of 24%. Interestingly, after removal of the bromide anion template, the catenane can act as a host to anions. It binds strongly to chloride and bromide, while binding to other anions such as iodide and acetate has not been observed.

In a more recent study the synthesis of pseudorotaxanes via interactions of a pyridine-containing macrocycle and different iodo-functionalized triazolium and iodo- and bromo-functionalized pyridinium components has been reported by Beer and co-workers.⁶⁸ Here, the pyridine-containing macrocycle acts as a halogen acceptor (XB acceptor), while the triazolium or pyridinium components act as a halogen donor (XB donor). In the same study, Beer and co-workers reported on the synthesis of a catenane. This synthesis was through a halogen-bonding interaction (C–I–N) between a halogen-functionalized pyridinium and a pyridine template. Ring closing to the catenane

was accomplished via olefin metathesis, using a Grubbs second-generation catalyst. Notably, no catenane formation was observed when the pyridinium building block lacked the iodo functionalization.

Diederich and co-workers reported recently the first synthesis of supramolecular cages via halogen-bonding interactions.⁶⁹ An example is cage **41**, which is shown in Scheme 23. The capsules assemble via interactions between four pyridine moieties functioning as XB acceptors and four 2,3,5,6-tetrafluoro-4-halophenyl moieties as XB donors. Both building blocks have a resorcin[4]arene-based backbone. Successful assemblies were observed for X = Br, I, while no cages could be obtained for X = F, Cl. Interestingly, **41** is able to form 1:2 host–guest complexes with 1,4-dioxane and 1,4-dithiane. This finding may lead to the use of **41** or a derivative as a molecular flask.

In addition to new concepts leading to cavity formation, new cavity designs are also of great importance. One approach is to synthesize cavities that have functional groups that are able to cooperate with each other. This is a challenging task, as it may cause the synthesis of less symmetrical systems.

Scheme 25. Synthesis of Macrocycle 46 via Imine Condensation Followed by Olefin Metathesis⁷³

As mentioned before, dynamic covalent chemistry (DCC) has already proven the potential to grant access to novel functionalized cavities. An example is cage **42**, which has been reported by Severin and co-workers (Scheme 24).⁷⁰ Via imine condensation and boronic acid–diol condensation **42** can be obtained in one pot from the building blocks 4-formylboronic acid (**43**, 6 equiv), pentaerythritol (**44**, 3 equiv), and 1,3,5-tris(aminomethyl)-2,4,6-triethylbenzene (**45**, 2 equiv). In addition, Mastalerz and co-workers demonstrated that cage interiors obtained via DCC can also be manipulated after the cavity has been synthesized.⁷¹

Heterosequenced cavities can be obtained via a combination of imine condensation and olefin metathesis. Zhang and co-workers reported the combination of these two transformations to obtain heterosequenced macrocycles such as **46** (Scheme 25) and cages.^{72,73} Thereby an assisted one-pot protocol was applied. The cavity synthesis started with the imine formation. Afterward the reaction mixture was exposed to vacuum in order to remove the water that had been formed during imine condensation. To avoid solvent removal, high-boiling 1,2,4-trichlorobenzene (TCB) was used. Once water had been removed, the cyclization or cage formation was accomplished via addition of the metathesis catalyst.

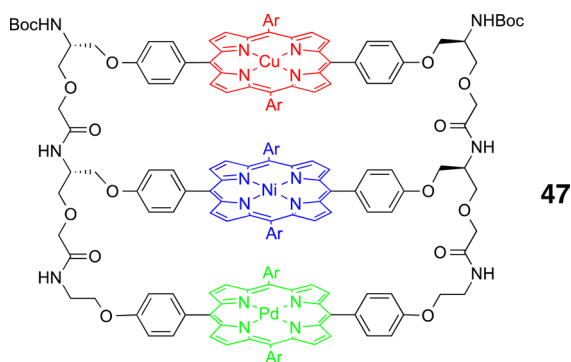
Tanaka and co-workers have established the selective assembly of the metal porphyrin trimer **47** (Figure 2).⁷⁴ Each porphyrin

low-yielding ring-closing reactions. However, due to their very precise functionalization, compounds such as **47** could be prototypes for multifunctionalized cavities, enabling the size-selective catalysis of multiple reactions in a one-pot tandem sequence. Such processes could avoid time- and cost-intensive purification methods.

An example of cooperativity between functional groups within a macrocycle has been demonstrated by Roemelt, Otte, and co-workers.⁷⁵ Macrocycle **48** has a pyridine and carboxylic acid functionalized interior. This Brønsted pair can interact with each other to form a hydrogen bond, resulting in a planar conformation, which is presumably due to intermolecular π -interactions poorly soluble. Through deprotonation the H bond is broken and **48-H**⁺ becomes readily soluble. This change comes presumably along with a change in conformation to a boat type conformation that has fewer π interactions (Scheme 26). As protonation and deprotonation are reversible, **48** can be seen as a pH-dependent molecular switch.

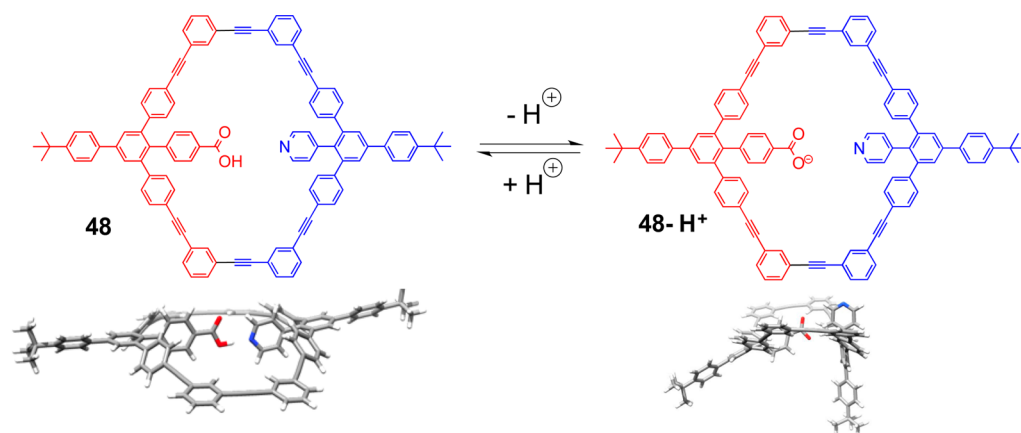
In addition to pH-active cavity **48**, a redox-active M_4L_2 cavity has recently been described by Goeb, Sallé, and co-workers.⁷⁶ The cavity assembles in acetonitrile via coordination of two tetradentate ligands to four different *cis*-Pd(dppf)(OTf)₂ (dppf = bis(diphenylphosphino)ferrocene) molecules. Coordination to the metals occurs via four pyridine moieties of the ligand. Moreover, the ligand offers a tetrathiafulvalene-functionalized backbone. The combination of these two groups allows the cavity to disassemble and reassemble reversibly upon chemical oxidation and reduction (Scheme 27). The disassembly upon oxidation occurs through use of a thianthrenium radical cation. Reduction is accomplished via reaction with tetrakis(dimethylamino)ethylene. Interestingly, disassembly of the cavity can also be accomplished after it has formed a 1:2 host–guest complex with B₁₂F₁₂²⁻. The opportunity to selectively assemble and disassemble a cavity may lead to molecular flasks that can be switched on and off.

Reek and co-workers reported very recently an example of how cooperativity between functional groups inside a cavity can be used for molecular flask catalysis.⁷⁷ They synthesized the Fujita-type $M_{12}L_{24}$ cage **49** that has multiple guanidinium binding sites at the cage interior (Scheme 28a). Fujita and co-workers reported previously on a $M_{12}L_{24}$ cage that has quaternary ammonium sites at the cage interior suitable to catalyze the polymerization of anionic monomers inside the cavity.⁷⁹ Acceleration of the polymerization and control of the molecular weights through the cage was observed by Fujita and co-workers.

Figure 2. Metal porphyrin trimer **47**.⁷⁴

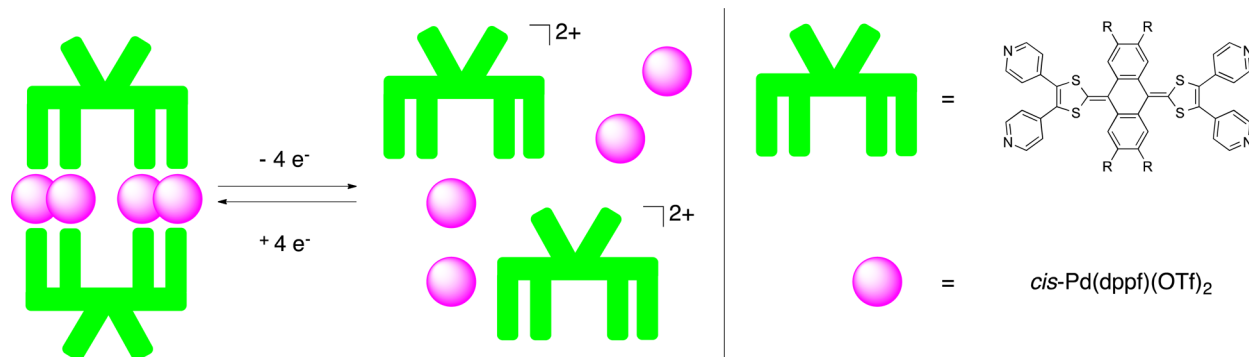
is functionalized with a different metal (Cu, Ni, Pd). Due to the chosen synthetic approach precise control of where each metal is in the porphyrin trimer is possible. In contrast to the examples described by Zhang, Severin, and Mastalerz, the synthesis of **47** does not proceed via DCC and requires therefore several

Scheme 26. Brønsted Pair Functionalized Macrocycle 48 as a pH-Dependent Molecular Switch (DFT-Optimized Geometries)^{4,75}



⁴Reproduced from ref 75. Copyright 2015 American Chemical Society.

Scheme 27. Illustration of a Redox-Controlled Cage Disassembly/Assembly⁷⁶



Cage 49 assembles via coordination of the dipyrindine building blocks to platinum.⁷⁷ Thereby each platinum ion is coordinated by four different ligands while each ligand coordinates to two different metal ions. The ligands have substituents pointing to the interior of the $M_{12}L_{24}$ cage 49, providing the guanidinium binding sites. These binding sites are able to coordinate to an encapsulated transition-metal complex. An example is the encapsulated gold complex $TPPMSAu^+$ ($TPPMS$ = triphenylphosphinomonosulfonate) resulting in the formation of host–guest complex 50 (Scheme 28b). In addition, these sites are able to bind to coencapsulated substrates, resulting in a preorganization of the substrate for catalytic conversion inside the cage. This strategy has been used for the gold-catalyzed cyclization of acetylenic acid to enol lactone in the presence of triethylamine (Scheme 28b). During this process the carboxylate binds to the guanidinium sites via hydrogen-bonding interactions (51). This preorganization enables the gold catalyst to activate the alkyne for an intramolecular cyclization, resulting in enol lactone formation (52). It has been shown that this preorganization results in increased reaction rates. Importantly, cavity 50 selectively converts the deprotonated acetylenic acid, while the protonated form has not been transformed. The results reported by Reek and co-workers may lead to the development of pH-controlled on/off switching of catalysis.

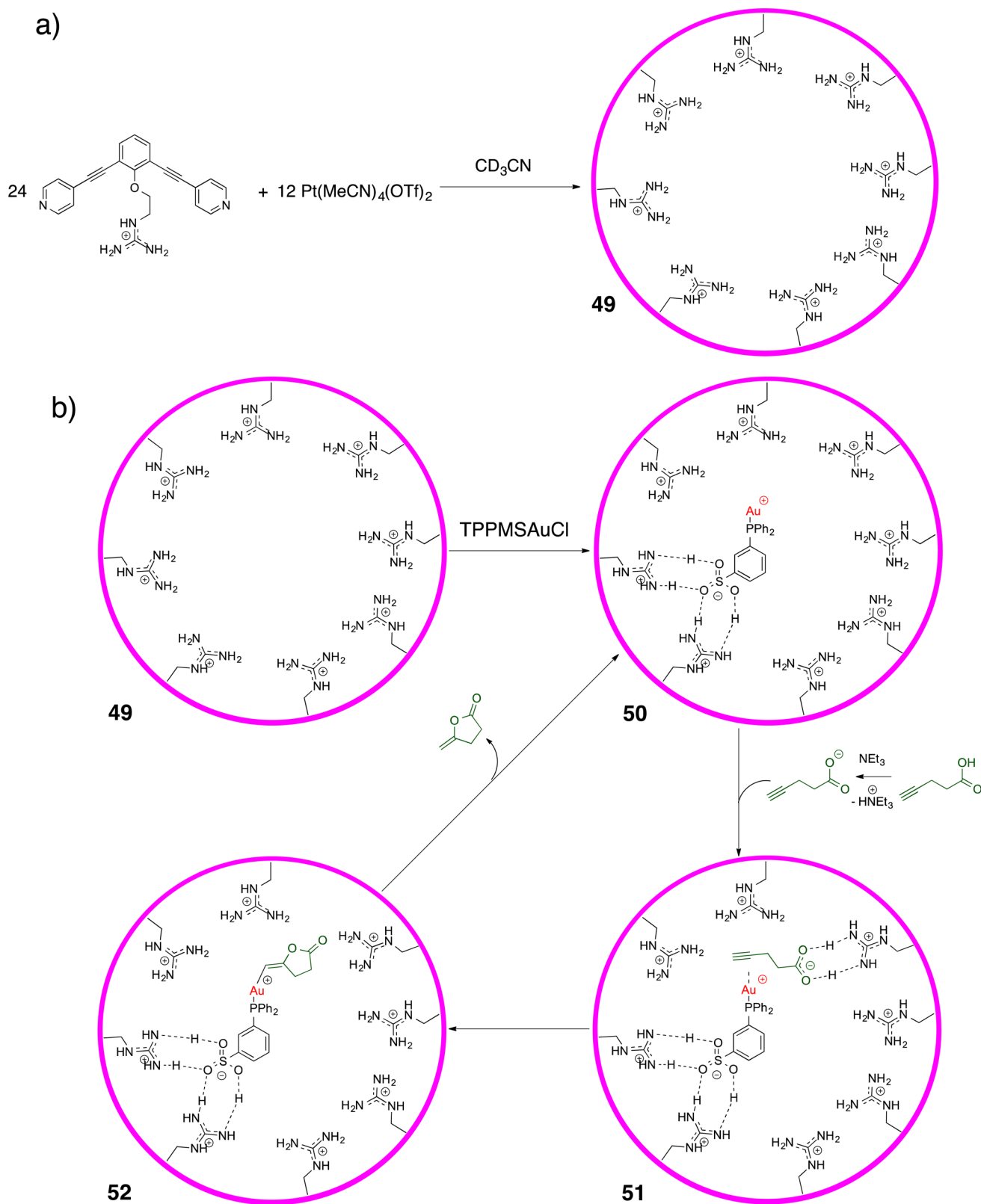
VI. CONCLUSION AND OUTLOOK

Materials such as metal–organic frameworks, polyoxometalates, and zeolites dominate size-selective catalysis at the moment.

However, the number of molecular flasks able to perform size-selective catalysis is continuously increasing. As shown here, molecular flasks can already catalyze many reactions in a size-selective manner, including olefin hydrogenation, epoxidation, and cyclopropanation, allyl alcohol isomerization, nucleophilic substitution, and hydroalkoxylation. However, in comparison to the extended portfolio of transformations of organic substrates, only a few of the known reactions can be catalyzed to date by size-selective molecular flasks. A future challenge will be to further expand the scope of reactions that can be performed. An example could be the development of molecular flasks that catalyze a size-selective olefin metathesis. The flask pores may separate the reagents on the basis of their size, while the confined space inside the cavity may lead to a different reaction product in comparison to the product that would be obtained from substrate conversion in the bulk reaction mixture. In addition, a way to increase the scope of reactions that can be catalyzed in a size-selective way would be to further combine size selectivity with stereoselectivity. A catalyst that could transform a single substrate from a mixture of substrates in a highly size-selective and enantioselective fashion would be of great value.

The development of new cavity designs will help to create new molecular flasks and thus enlarge the scope of size-selective transformations within molecular flasks. Cavity design via DCC is a prominent example of a new concept that enlarges the library of reported cavities dramatically.⁸⁰ In addition, a better understanding and control of encapsulated species will also lead

Scheme 28. (a) Schematic Synthesis of Cage 49 and (b) Schematic Representation of the 50-Catalyzed Cyclization of Acetylenic Acid⁷⁷



to new molecular flasks. Examples of recent contributions have been given by Nitschke and co-workers, who studied the solvent effects upon guest binding.⁸¹ Moreover, the control over binding of an encapsulated guest to the host via external

binding of reagents to two distinct allosteric sites has also been described.⁸²

Increased selectivity for molecular flasks will also be of great importance toward their further application. Reported

size-selective transformations catalyzed by molecular flasks often describe only competition experiments between two substrates that differ dramatically in size. However, competition experiments for chemical transformations of more complicated mixtures have barely been reported. In addition, high size selectivity has come so far mostly at the cost of a small substrate scope, while catalysts with a broader substrate scope result often in moderate size selectivities.

In addition to the development of new size-selective reactions and the aim of developing systems that can distinguish between more than two substrates comes the goal for an industrial application of size-selective molecular flasks. One possible application could be their use in the size-selective transformation of substrates in crude oil or biomass. As catalysts for crude oil and biomass conversion need to perform many turnovers under often harsh conditions, molecular flasks might currently be too cost intensive for use as catalysts. However, Mukherjee and co-workers reported on molecular flasks that are heterogeneous catalysts. Those can be recycled several times while remaining catalytically active.^{13f,19d} In addition, the knowledge gained through the precise design of molecular flasks might be beneficial for the design of other types of size-selective catalysts such as MOFs and COFs (covalent organic frameworks). A further application of size-selective molecular flasks could lie in the synthesis of pharmaceuticals or fine chemicals. As pharmaceuticals are often compounds of very high value, the high prices of the molecular flasks would be less of a concern in comparison to the biomass or crude oil conversion. This approach could become interesting in particular in cases where the molecular flasks also become highly stereoselective catalysts.

Overall many efforts are currently being spent on the chemistry of functionalized cavities. This results in a continuous output of very important findings. These will also translate to the field of molecular flasks, which will most certainly result in many very exciting developments and applications.

AUTHOR INFORMATION

Corresponding Author

*E-mail for M.O.: m.otte@uu.nl.

Notes

The author declares no competing financial interest.

ACKNOWLEDGMENTS

M.O. thanks the sustainability scheme of Utrecht University for funding. Robertus J. M. Klein Gebbink is acknowledged for fruitful discussions and proofreading.

ABBREVIATIONS

COF, covalent organic framework; Cp*, C₅Me₅; dppf, bis(diphenylphosphino)ferrocene; DPyP, dipyrroline-porphyrin; dr, diastereomeric ratio; ee, enantiomeric excess; MOF, metal-organic framework; TCB, 1,2,4-trichlorobenzene; THF, tetrahydrofuran; TOF, turnover frequency; tim, 1,2,4,5-tetrakis-(1-imidazolyl)benzene; timb, 1,3,5-tris(1-imidazolyl)benzene; tmen, N,N,N',N'-tetramethylethylenediamine; TPP, tetraphenylporphyrin; TPPMS, triphenylphosphinomonosulfonate

REFERENCES

- (1) Cram, D. J.; Bauer, R. H. *J. Am. Chem. Soc.* **1959**, *81*, 5971–5977.
- (2) Lehn, J. M. *Acc. Chem. Res.* **1978**, *11*, 49–57.
- (3) Pedersen, C. J. *J. Am. Chem. Soc.* **1967**, *89*, 7017–7036.

- (4) Vögtle, F.; Weber, E. *Angew. Chem., Int. Ed. Engl.* **1974**, *13*, 814–816.
- (5) Rebek, J. J.; Heinz, T.; Rudkevich, D. M. *Nature* **1998**, *394*, 764–766.
- (6) Stang, P. J.; Olenyuk, B.; Whiteford, J. A.; Fechtenkötter, A. *Nature* **1999**, *398*, 796–799.
- (7) Fujita, M.; Takeda, N.; Umemoto, K.; Yamaguchi, K. *Nature* **1999**, *398*, 794–796.
- (8) (a) Anderson, S.; Anderson, H. L.; Bashall, A.; McPartlin, M.; Sanders, J. K. M. *Angew. Chem., Int. Ed. Engl.* **1995**, *34*, 1096–1099. (b) Liu, P.; Hisamune, Y.; Peeks, M. D.; Odell, B.; Gong, J. Q.; Herz, L. M.; Anderson, H. L. *Angew. Chem., Int. Ed.* **2016**, *55*, 8358–8362.
- (9) (a) Black, S. P.; Stefankiewicz, A. R.; Smulders, M. M. J.; Sattler, D.; Schalley, C. A.; Nitschke, J. R.; Sanders, J. K. M. *Angew. Chem., Int. Ed.* **2013**, *52*, 5749–5752. (b) Freye, S.; Michel, R.; Stalke, D.; Pawliczek, M.; Frauendorf, H.; Clever, G. H. *J. Am. Chem. Soc.* **2013**, *135*, 8476–8479. (c) Leigh, D. A.; Pritchard, R. G.; Stephens, A. J. *Nat. Chem.* **2014**, *6*, 978–982. (d) Beves, J. E.; Danon, J. J.; Leigh, D. A.; Lemonnier, J.-F.; Victoria-Yrezabal, I. J. *Angew. Chem., Int. Ed.* **2015**, *54*, 7555–7559.
- (10) (a) Zhang, C.; Wang, Q.; Long, H.; Zhang, W. *J. Am. Chem. Soc.* **2011**, *133*, 20995–21001. (b) Jiao, D.; Biedermann, F.; Scherman, O. A. *Org. Lett.* **2011**, *13*, 3044–3047. (c) Lippe, J.; Mazik, M. *J. Org. Chem.* **2013**, *78*, 9013–9020. (d) Turega, S.; Whitehead, M.; Hall, B. R.; Meijer, A. J. H. M.; Hunter, C. A.; Ward, M. D. *Inorg. Chem.* **2013**, *52*, 1122–1132. (e) Ronson, T. K.; Giri, C.; Beyeh, N. K.; Minkinen, A.; Topić, F.; Holstein, J. J.; Rissanen, K.; Nitschke, J. R. *Chem. - Eur. J.* **2013**, *19*, 3374–3382. (f) Sun, X.; James, T. D. *Chem. Rev.* **2015**, *115*, 8001–8037. (g) Mooibroek, T. J.; Casas-Solvas, J. M.; Harniman, R. L.; Renney, C. M.; Carter, T. S.; Crump, M. P.; Davis, A. P. *Nat. Chem.* **2015**, *8*, 69–74. (h) Rios, P.; Carter, T. S.; Mooibroek, T. J.; Crump, M. P.; Lisbjerg, M.; Pittelkow, M.; Supekar, N. T.; Boons, G.-J.; Davis, A. P. *Angew. Chem., Int. Ed.* **2016**, *55*, 3387–3392.
- (11) (a) Tozawa, T.; Jones, J. T. A.; Swamy, S. I.; Jiang, S.; Adams, D. J.; Shakespeare, S.; Clowes, R.; Bradshaw, D.; Hasell, T.; Chong, S. Y.; Tang, C.; Thompson, S.; Parker, J.; Trewin, A.; Bacsa, J.; Slawin, A. M. Z.; Steiner, A.; Cooper, A. I. *Nat. Mater.* **2009**, *8*, 973–978. (b) Jin, Y.; Voss, B. A.; Jin, A.; Long, H.; Noble, R. D.; Zhang, W. *J. Am. Chem. Soc.* **2011**, *133*, 6650–6658. (c) Avellaneda, A.; Valente, P.; Burgun, A.; Evans, J. D.; Markwell-Heys, A. W.; Rankine, D.; Nielsen, D. J.; Hill, M. R.; Sumby, C. J.; Doonan, C. J. *Angew. Chem., Int. Ed.* **2013**, *52*, 3746–3749. (d) Chen, L.; Reiss, P. S.; Chong, S. Y.; Holden, D.; Jelfs, K. E.; Hasell, T.; Little, M. A.; Kewley, A.; Briggs, M. E.; Stephenson, A.; Thomas, K. M.; Armstrong, J. A.; Bell, J.; Busto, J.; Noel, R.; Liu, J.; Strachan, D. M.; Thallapally, P. K.; Cooper, A. I. *Nat. Mater.* **2014**, *13*, 954–960. (e) Janczak, J.; Prochowicz, D.; Lewiński, J.; Fairen-Jimenez, D.; Bereta, T.; Lisowski, J. *Chem. - Eur. J.* **2016**, *22*, 598–609.
- (12) (a) Asakawa, M.; Ashton, P. R.; Balzani, V.; Credi, A.; Hamers, C.; Mattersteig, G.; Montalti, M.; Shipway, A. N.; Spencer, N.; Stoddart, J. F.; Tolley, M. S.; Venturi, M.; White, A. J. P.; Williams, D. J. *Angew. Chem., Int. Ed.* **1998**, *37*, 333–337. (b) Collier, C. P.; Mattersteig, G.; Wong, E. W.; Luo, Y.; Beverly, K.; Sampaio, J.; Raymo, F. M.; Stoddart, J. F.; Heath, J. R. *Science* **2000**, *289*, 1172–1175. (c) Liu, Y.; Flood, A. H.; Stoddart, J. F. *J. Am. Chem. Soc.* **2004**, *126*, 9150–9151. (d) Huang, Y.-L.; Hung, W.-C.; Lai, C.-C.; Liu, Y.-H.; Peng, S.-M.; Chiu, S.-H. *Angew. Chem., Int. Ed.* **2007**, *46*, 6629–6633.
- (13) (a) Ziegler, M.; Brumaghim, J. L.; Raymond, K. N. *Angew. Chem., Int. Ed.* **2000**, *39*, 4119–4121. (b) Dong, V. M.; Fiedler, D.; Carl, B.; Bergman, R. G.; Raymond, K. N. *J. Am. Chem. Soc.* **2006**, *128*, 14464–14465. (c) Mal, P.; Breiner, B.; Rissanen, K.; Nitschke, J. R. *Science* **2009**, *324*, 1697–1699. (d) McCaffrey, R.; Long, H.; Jin, Y.; Sander, A.; Park, W.; Zhang, W. *J. Am. Chem. Soc.* **2014**, *136*, 1782–1785. (e) Galan, A.; Ballester, P. *Chem. Soc. Rev.* **2016**, *45*, 1720–1737. (f) Mondal, B.; Acharyya, K.; Howlader, P.; Mukherjee, P. S. *J. Am. Chem. Soc.* **2016**, *138*, 1709–1716.
- (14) For reviews on molecular flasks see: (a) Yoshizawa, M.; Klosterman, J. K.; Fujita, M. *Angew. Chem., Int. Ed.* **2009**, *48*, 3418–

3438. (b) Wiester, J. M.; Ulmann, P. A.; Mirkin, C. A. *Angew. Chem., Int. Ed.* **2011**, *50*, 114–137. (c) Leenders, S. H. A. M.; Gramage-Doria, R.; de Bruin, B.; Reek, J. N. H. *Chem. Soc. Rev.* **2015**, *44*, 433–448.
- (15) Kang, J.; Santamaría, J.; Hilmersoon, G.; Rebek, J. J. *J. Am. Chem. Soc.* **1998**, *120*, 7389–7390.
- (16) (a) Yoshizawa, M.; Tamura, M.; Fujita, M. *Science* **2006**, *312*, 251–254. (b) Murase, T.; Horiuchi, S.; Fujita, M. *J. Am. Chem. Soc.* **2010**, *132*, 2866–2867. (c) Cavarzan, A.; Scarso, A.; Sgarbossa, P.; Strukul, G.; Reek, J. N. H. *J. Am. Chem. Soc.* **2011**, *133*, 2848–2851. (d) Gramage-Doria, R.; Hessels, J.; Leenders, S. H. M.; Tröppner, O.; Dürr, M.; Ivanović-Burmazović, I.; Reek, J. N. H. *Angew. Chem., Int. Ed.* **2014**, *53*, 13380–13384.
- (17) Dalton, D. M.; Ellis, S. R.; Nichols, E. M.; Mathies, R. A.; Toste, F. D.; Bergman, R. G.; Raymond, K. N. *J. Am. Chem. Soc.* **2015**, *137*, 10128–10131.
- (18) (a) Thordarson, P.; Bijsterveld, E. J. A.; Rowan, A. E.; Nolte, R. J. M. *Nature* **2003**, *424*, 915–918. (b) Brown, C. J.; Bergman, R. G.; Raymond, K. N. *J. Am. Chem. Soc.* **2009**, *131*, 17530–17531. (c) Jouffroy, M.; Gramage-Doria, R.; Armspach, D.; Sémeril, D.; Oberhauser, W.; Matt, D.; Toupet, L. *Angew. Chem., Int. Ed.* **2014**, *53*, 3937–3940. (d) García-Simón, C.; Gramage-Doria, R.; Raoofmoghaddam, S.; Parella, T.; Costas, M.; Ribas, X.; Reek, J. N. H. *J. Am. Chem. Soc.* **2015**, *137*, 2680–2687.
- (19) (a) Walter, C. J.; Anderson, H. L.; Sanders, J. K. M. *J. Chem. Soc., Chem. Commun.* **1993**, 458–460. (b) Clyde-Watson, Z.; Vidal-Ferran, A.; Twyman, L. J.; Walter, C. J.; McCallien, D. W. J.; Fanni, S.; Bampos, N.; Wylie, R. S.; Sander, J. K. M. *New J. Chem.* **1998**, *22*, 493–502. (c) Chen, J.; Rebek, J. J. *Org. Lett.* **2002**, *4*, 327–329. (d) Howlader, P.; Das, P.; Zangrando, E.; Mukherjee, P. S. *J. Am. Chem. Soc.* **2016**, *138*, 1668–1676.
- (20) Otte, M.; Kuijpers, P. F.; Troepner, O.; Ivanović-Burmazović, I.; Reek, J. N. H.; de Bruin, B. *Chem. - Eur. J.* **2013**, *19*, 10170–10178.
- (21) Examples of size-selective transformations with materials such as metal–organic frameworks, zeolites, and covalent organic frameworks: (a) Qiu, L.-G.; Xie, A.-J.; Zhang, L.-D. *Adv. Mater.* **2005**, *17*, 689–692. (b) Horike, S.; Dincă, M.; Tamaki, K.; Long, J. R. *J. Am. Chem. Soc.* **2008**, *130*, 5854–5855. (c) Laursen, A. B.; Højholt, K. T.; Lundegaard, L. F.; Simonsen, S. B.; Helveg, S.; Schüth, F.; Paul, M.; Grunwaldt, J.-D.; Kegnæs, S.; Christensen, C. H.; Egeblad, K. *Angew. Chem., Int. Ed.* **2010**, *49*, 3504–3507. (d) Mizuno, N.; Uchida, S.; Kamata, K.; Ishimoto, R.; Nojima, S.; Yonehara, K.; Sumida, Y. *Angew. Chem., Int. Ed.* **2010**, *49*, 9972–9976. (e) Roberts, J. M.; Fini, B. M.; Sarjeant, A. A.; Farha, O. K.; Hupp, J. T.; Scheidt, K. A. *J. Am. Chem. Soc.* **2012**, *134*, 3334–3337. (f) Han, Q.; He, C.; Zhao, M.; Qi, B.; Niu, J.; Duan, C. *J. Am. Chem. Soc.* **2013**, *135*, 10186–10189. (g) Qiao, Z.-A.; Zhang, P.; Chai, S.-H.; Chi, M.; Veith, G. M.; Gallego, N. C.; Kidder, M.; Dai, S. *J. Am. Chem. Soc.* **2014**, *136*, 11260–11263. (h) Zhang, W.; Lu, G.; Cui, C.; Liu, Y.; Li, S.; Yan, W.; Xing, C.; Chi, Y. R.; Yang, Y.; Huo, F. *Adv. Mater.* **2014**, *26*, 4056–4060.
- (22) Recent examples of cavities that are based on metal–ligand coordination: (a) Riddell, I. A.; Smulders, M. M.; Clegg, J. K.; Hristova, Y. R.; Breiner, B.; Thoburn, J. D.; Nitschke, J. R. *Nat. Chem.* **2012**, *4*, 751–756. (b) Li, S.; Huang, J.; Cook, T. R.; Pollock, J. B.; Kim, H.; Chi, K.-W.; Stang, P. J. *J. Am. Chem. Soc.* **2013**, *135*, 2084–2087. (c) Bolliger, J. L.; Belenguer, A. M.; Nitschke, J. R. *Angew. Chem., Int. Ed.* **2013**, *52*, 7958–7962. (d) Li, S.; Huang, J.; Zhou, F.; Cook, T. R.; Xuzhou, Y.; Ye, Y.; Zhu, B.; Zheng, B.; Stang, P. J. *J. Am. Chem. Soc.* **2014**, *136*, 5908–5911. (e) Zhu, R.; Lübben, J.; Dittrich, B.; Clever, G. H. *Angew. Chem., Int. Ed.* **2015**, *54*, 2796–2800. (f) Löffler, S.; Lübben, J.; Krause, L.; Stalke, D.; Dittrich, B.; Clever, G. H. *J. Am. Chem. Soc.* **2015**, *137*, 1060–1063.
- (23) Recent overview on cavities that are based on metal–ligand coordination: (a) Amouri, H.; Desmaret, C.; Moussa, J. *Chem. Rev.* **2012**, *112*, 2015–2041. (b) Cook, T. R.; Stang, P. J. *Chem. Rev.* **2015**, *115*, 7001–7045.
- (24) Recent overview on catalysis in metal–organic coordination hosts: Brown, C. J.; Toste, F. D.; Bergman, R. G.; Raymond, K. N. *Chem. Rev.* **2015**, *115*, 3012–3035.
- (25) (a) Yoshizawa, M.; Kusukawa, T.; Fujita, M.; Sakamoto, S.; Yamaguchi, K. *J. Am. Chem. Soc.* **2001**, *123*, 10454–10459. (b) Yoshizawa, M.; Takeyama, Y.; Kusukawa, T.; Fujita, M. *Angew. Chem., Int. Ed.* **2002**, *41*, 1347–1349. (c) Yoshizawa, M.; Miyagi, S.; Kawano, M.; Ishiguro, K.; Fujita, M. *J. Am. Chem. Soc.* **2004**, *126*, 9172–9173. (d) Nishioka, Y.; Yamaguchi, T.; Yoshizawa, M.; Fujita, M. *J. Am. Chem. Soc.* **2007**, *129*, 7000–7001.
- (26) (a) Kaphan, D. M.; Levin, M. D.; Bergman, R. G.; Raymond, K. N.; Toste, F. D. *Science* **2015**, *350*, 1235–1238. (b) Kaphan, D. M.; Toste, F. D.; Bergman, R. G.; Raymond, K. N. *J. Am. Chem. Soc.* **2015**, *137*, 9202–9205.
- (27) Merlau, M. L.; del Pilar Mejia, M.; Nguyen, S. T.; Hupp, J. T. *Angew. Chem., Int. Ed.* **2001**, *40*, 4239–4242.
- (28) Lee, S. J.; Mulfort, K. L.; Zuo, X.; Goshe, A. J.; Wesson, P. J.; Nguyen, S. T.; Hupp, J. T.; Tiede, D. M. *J. Am. Chem. Soc.* **2008**, *130*, 836–838.
- (29) Lee, S. J.; Cho, S.-H.; Mulfort, K. L.; Tiede, D. M.; Hupp, J. T.; Nguyen, S. T. *J. Am. Chem. Soc.* **2008**, *130*, 16828–16829.
- (30) Caulder, D. L.; Powers, R. E.; Parac, T. N.; Raymond, K. N. *Angew. Chem., Int. Ed.* **1998**, *37*, 1840–1843.
- (31) Leung, D. H.; Fiedler, D.; Bergman, R. G.; Raymond, K. N. *Angew. Chem., Int. Ed.* **2004**, *43*, 963–966.
- (32) Leung, D. H.; Bergman, R. G.; Raymond, K. N. *J. Am. Chem. Soc.* **2006**, *128*, 9781–9797.
- (33) Pluth, M. D.; Bergman, R. G.; Raymond, K. N. *Science* **2007**, *316*, 85–88.
- (34) Leung, D. H.; Bergman, R. G.; Raymond, K. N. *J. Am. Chem. Soc.* **2007**, *129*, 2746–2747.
- (35) Wu, X.; He, C.; Wu, X.; Qu, S.; Duan, C. *Chem. Commun.* **2011**, *47*, 8415–8417.
- (36) Wang, J.; He, C.; Wu, P.; Wang, J.; Duan, C. *J. Am. Chem. Soc.* **2011**, *133*, 12402–12405.
- (37) Jiao, Y.; Wang, J.; Wu, P.; Zhao, L.; He, C.; Zhang, J.; Duan, C. *Chem. - Eur. J.* **2014**, *20*, 2224–2231.
- (38) Murase, T.; Nishijima, Y.; Fujita, M. *J. Am. Chem. Soc.* **2012**, *134*, 162–164.
- (39) Samanta, D.; Mukherjee, S.; Patil, Y. P.; Mukherjee, P. S. *Chem. - Eur. J.* **2012**, *18*, 12322–12329.
- (40) Samanta, D.; Mukherjee, P. S. *Chem. Commun.* **2013**, *49*, 4307–4309.
- (41) Meng, W.; Breiner, B.; Rissanen, K.; Thoburn, J. D.; Clegg, J. K.; Nitschke, J. R. *Angew. Chem., Int. Ed.* **2011**, *50*, 3479–3483.
- (42) Otte, M.; Kuijpers, P. F.; Troepner, O.; Ivanović-Burmazović, I.; Reek, J. N. H.; de Bruin, B. *Chem. - Eur. J.* **2014**, *20*, 4880–4884.
- (43) Kuijpers, P. F.; Otte, M.; Dürr, M.; Ivanović-Burmazović, I.; Reek, J. N. H.; de Bruin, B. *ACS Catal.* **2016**, *6*, 3106–3112.
- (44) Wyler, R.; Mendoza, J.; Rebek, J. J. *Angew. Chem., Int. Ed. Engl.* **1993**, *32*, 1699–1701.
- (45) (a) Branda, N.; Wyler, R.; Rebek, J. J. *Science* **1994**, *263*, 1267–1268. (b) Rivera, J. M.; Martín, T.; Rebek, J. J. *J. Am. Chem. Soc.* **2001**, *123*, 5213–5220.
- (46) For examples see: (a) Vysotsky, M. O.; Thondorf, I.; Böhmer, V. *Angew. Chem., Int. Ed.* **2000**, *39*, 1264–1267. (b) Gibb, C. L. D.; Gibb, B. C. *J. Am. Chem. Soc.* **2004**, *126*, 11408–11409. (c) Corbellini, F.; van Leeuwen, F. W. B.; Beijleveld, H.; Kooijman, H.; Spek, A. L.; Verboom, W.; Crego-Calama, M.; Reinhoudt, D. N. *New J. Chem.* **2005**, *29*, 243–248. (d) Montoro-García, C.; Camacho-García, J.; López-Pérez, A. M.; Bilbao, N.; Romero-Pérez, S.; Mayoral, M. J.; González-Rodríguez, D. *Angew. Chem., Int. Ed.* **2015**, *54*, 6780–6784. (e) Račkauskaitė, D.; Gegevičius, R.; Matsuo, Y.; Wärnmark, K.; Orentas, E. *Angew. Chem., Int. Ed.* **2016**, *55*, 208–212.
- (47) Kang, J.; Rebek, J. J. *Nature* **1997**, *385*, 50–52.
- (48) (a) Kaanumalle, L. S.; Gibb, C. L. D.; Gibb, B. C.; Ramamurthy, V. *J. Am. Chem. Soc.* **2004**, *126*, 14366–14367. (b) Ramamurthy, V. *Acc. Chem. Res.* **2015**, *48*, 2904–2917.
- (49) Atwood, J. L.; MacGillivray, L. R. *Nature* **1997**, *389*, 469–472.
- (50) Zhang, Q.; Tiefenbacher, K. *J. Am. Chem. Soc.* **2013**, *135*, 16213–16219.
- (51) Zhang, Q.; Tiefenbacher, K. *Nat. Chem.* **2015**, *7*, 197–202.

- (52) Catti, L.; Tiefenbacher, K. *Chem. Commun.* **2015**, 51, 892–894.
- (53) Bianchini, G.; La Sorella, G.; Canever, N.; Scarso, A.; Strukul, G. *Chem. Commun.* **2013**, 49, 5322–5324.
- (54) La Sorella, G.; Sporni, L.; Strukul, G.; Scarso, A. *ChemCatChem* **2015**, 7, 291–296.
- (55) Giust, S.; La Sorella, G.; Sporni, L.; Strukul, G.; Scarso, A. *Chem. Commun.* **2015**, 51, 1658–1661.
- (56) For an overview see: (a) Mastalerz, M. *Angew. Chem., Int. Ed.* **2010**, 49, 5042–5053. (b) Hunt, R. A. R.; Otto, S. *Chem. Commun.* **2011**, 47, 847–858. (c) Jin, Y.; Yu, C.; Denman, R. J.; Zhang, W. *Chem. Soc. Rev.* **2013**, 42, 6634–6654. (d) Jin, Y.; Wang, Q.; Taynton, P.; Zhang, W. *Acc. Chem. Res.* **2014**, 47, 1575–1586.
- (57) For examples see: (a) Chatelet, B.; Dufaud, V.; Dutasta, J.-P.; Martinez, A. *J. Org. Chem.* **2014**, 79, 8684–8688. (b) Chatelet, B.; Joucla, L.; Dutasta, J.-P.; Martinez, A.; Dufaud, V. *Chem. - Eur. J.* **2014**, 20, 8571–8574. (c) Lee, Y.; Sloane, F. T.; Blondin, G.; Abboud, K. A.; Garcia-Serres, R.; Murray, L. J. *Angew. Chem., Int. Ed.* **2015**, 54, 1499–1503. (d) Ermert, D. M.; Ghiviriga, I.; Catalano, V. J.; Shearer, J.; Murray, L. J. *Angew. Chem., Int. Ed.* **2015**, 54, 7047–7050. (e) Sun, J.-K.; Zhan, W.-W.; Akita, T.; Xu, Q. *J. Am. Chem. Soc.* **2015**, 137, 7063–7066. (f) Mondal, B.; Acharyya, K.; Howlader, P.; Mukherjee, P. S. *J. Am. Chem. Soc.* **2016**, 138, 1709–1716.
- (58) Cook, B. R.; Reinert, T. J.; Suslick, K. S. *J. Am. Chem. Soc.* **1986**, 108, 7281–7286.
- (59) Collman, J. P.; Zhang, X.; Hembre, R. T.; Brauman, J. I. *J. Am. Chem. Soc.* **1990**, 112, 5356–5357.
- (60) Cacciapaglia, R.; Di Stefano, S.; Mandolini, L. *J. Org. Chem.* **2002**, 67, 521–525.
- (61) Cacciapaglia, R.; Casnati, A.; Mandolini, L.; Reinhoudt, D. N.; Salvio, R.; Sartori, A.; Ungaro, R. *J. Org. Chem.* **2005**, 70, 5398–5402.
- (62) Crooks, R. M.; Zhao, M.; Sun, L.; Chechik, V.; Yeung, L. K. *Acc. Chem. Res.* **2001**, 34, 181–190.
- (63) Niu, Y.; Yeung, L. K.; Crooks, R. M. *J. Am. Chem. Soc.* **2001**, 123, 6840–6846.
- (64) Ueno, T.; Suzuki, M.; Goto, T.; Matsumoto, T.; Nagayama, K.; Watanabe, Y. *Angew. Chem., Int. Ed.* **2004**, 43, 2527–2530.
- (65) Zhang, S.; Zhao, Y. *ACS Nano* **2011**, 5, 2637–2646.
- (66) Lee, L.-C.; Zhao, Y. *Org. Lett.* **2012**, 14, 784–787.
- (67) Caballero, A.; Zapata, F.; White, N. G.; Costa, P. J.; Félix, V.; Beer, P. D. *Angew. Chem., Int. Ed.* **2012**, 51, 1876–1880.
- (68) Gilday, L. C.; Lang, T.; Caballero, A.; Costa, P. J.; Félix, V.; Beer, P. D. *Angew. Chem., Int. Ed.* **2013**, 52, 4356–4360.
- (69) Dumelele, O.; Trapp, N.; Diederich, F. *Angew. Chem., Int. Ed.* **2015**, 54, 12339–12344.
- (70) İçli, B.; Christinat, N.; Tönnemann, J.; Schüttler, C.; Scopelliti, R.; Severin, K. *J. Am. Chem. Soc.* **2009**, 131, 3154–3155.
- (71) Schneider, M. W.; Oppel, I. M.; Griffin, A.; Mastalerz, M. *Angew. Chem., Int. Ed.* **2013**, 52, 3611–3615.
- (72) Okochi, K. D.; Jin, Y.; Zhang, W. *Chem. Commun.* **2013**, 49, 4418–4420.
- (73) Okochi, K. D.; Han, G. S.; Aldridge, I. M.; Zhang, W. *Org. Lett.* **2013**, 15, 4296–4299.
- (74) Yamada, Y.; Kubota, T.; Nishio, M.; Tanaka, K. *J. Am. Chem. Soc.* **2014**, 136, 6505–6509.
- (75) Vliegthart, A. B.; Welling, F. A. L.; Roemelt, M.; Klein Gebbink, R. J. M.; Otte, M. *Org. Lett.* **2015**, 17, 4172–4175.
- (76) Croué, V.; Goeb, S.; Szalóki, G.; Allain, M.; Sallé, M. *Angew. Chem., Int. Ed.* **2016**, 55, 1746–1750.
- (77) Wang, Q.-Q.; Gonell, S.; Leenders, S. H. M.; Dürr, M.; Ivanović-Burmazović, I.; Reek, J. N. H. *Nat. Chem.* **2016**, 8, 225–230.
- (78) Tominaga, M.; Suzuki, K.; Murase, T.; Fujita, M. *J. Am. Chem. Soc.* **2005**, 127, 11950–11951.
- (79) Kikuchi, T.; Murase, T.; Sato, S.; Fujita, M. *Supramol. Chem.* **2008**, 20, 81–94.
- (80) Examples of cavities synthesized via DCC: (a) Otto, S.; Furlan, R. L. E.; Sanders, J. K. M. *Science* **2002**, 297, 590–593. (b) Mastalerz, M.; Schneider, M. W.; Oppel, I. M.; Presly, O. *Angew. Chem., Int. Ed.* **2011**, 50, 1046–1051. (c) Otto, S. *Acc. Chem. Res.* **2012**, 45, 2200–2210. (d) Wang, Q.; Zhang, C.; Noll, B. C.; Long, H.; Jin, Y.; Zhang, W. *Angew. Chem., Int. Ed.* **2014**, 53, 10663–10667. (e) Wang, Q.; Yu, C.; Long, H.; Du, Y.; Jin, Y.; Zhang, W. *Angew. Chem., Int. Ed.* **2015**, 54, 7550–7554. (f) Hong, S.; Rohman, R.; Jia, J.; Kim, Y.; Moon, D.; Kim, Y.; Ko, Y. H.; Lee, E.; Kim, K. *Angew. Chem., Int. Ed.* **2015**, 54, 13241–13244. (g) Lee, S.; Yang, A.; Money Penny, T. P.; Moore, J. S. *J. Am. Chem. Soc.* **2016**, 138, 2182–2185. (h) Wang, Q.; Yu, C.; Zhang, C.; Long, H.; Azarnoush, S.; Jin, Y.; Zhang, W. *Chem. Sci.* **2016**, 7, 3370–3376.
- (81) Bolliger, J. L.; Ronson, T. K.; Ogawa, M.; Nitschke, J. R. *J. Am. Chem. Soc.* **2014**, 136, 14545–14553.
- (82) Ramsay, W. J.; Nitschke, J. R. *J. Am. Chem. Soc.* **2014**, 136, 7038–7043.